MATHEMATICAL ENGINEERING
TECHNICAL REPORTS

Design of Compliant Mechanisms with Standardized Beam Elements via Mixed-Integer Programming

Shiro OZAKI and Yoshihiro KANNO

METR 2015–08 March 2015

DEPARTMENT OF MATHEMATICAL INFORMATICS
GRADUATE SCHOOL OF INFORMATION SCIENCE AND TECHNOLOGY
THE UNIVERSITY OF TOKYO
BUNKYO-KU, TOKYO 113-8656, JAPAN

WWW page: http://www.keisu.t.u-tokyo.ac.jp/research/techrep/index.html

Design of Compliant Mechanisms with Standardized Beam Elements via Mixed-Integer Programming

Shiro Ozaki [†], Yoshihiro Kanno [‡]

Department of Mathematical Informatics,
University of Tokyo, Tokyo 113-8656, Japan

Abstract

Design of compliant mechanisms requires both giving a structure flexibility that produces the kinematic performance and assuring stiffness to resist against structural failure. Presented in this paper is a mixed-integer programming approach to design optimization of a compliant mechanism realized as a frame structure consisting of standardized beam elements. In the optimization problem, the local stress constraints are addressed directly and the displacement of the output node is maximized. As an element-connectivity discretization, each member of the ground structure is divided into three components, one long member and two short joint elements, and the dimensions of cross-sections of joint elements are considered discrete design variables. Accordingly, the optimal solution of the proposed formulation contains no hinge-like region. The design optimization problem is formulated as a mixed-integer linear programming problem and, hence, can be solved globally by using an existing algorithm such as a branch-and-cut method. For solving large-scale problems we propose a heuristic local search, in which mixed-integer linear programming subproblems are solved sequentially. Numerical examples demonstrate that frame structures that can serve as compliant mechanisms are obtained by the proposed method.

Keywords

Compliant mechanism; topology optimization; integer programming; element-connectivity parameterization; stress constraint.

1 Introduction

Optimal design of compliant mechanisms has been one of substantial and promising subjects of structural optimization. A compliant mechanism consists of single piece and, hence, does not require the assembly process and lubrication. Also, compliant mechanisms have capability of elastic recovery. Because of these properties, complaint mechanisms are considered advantageous over conventional link mechanisms. Design optimization problems of compliant mechanisms have been mostly attacked within the framework of continuum-based topology optimization; see, e.g., [5, 13,

[†]Department of Mathematical Informatics, Graduate School of Information Science and Technology, University of Tokyo, Tokyo 113-8656, Japan. Present address: NTT DATA Corporation. 3-3-3 Toyosu, Koto, Tokyo 135-6033, Japan.

[‡]Corresponding author. Department of Mathematical Informatics, Graduate School of Information Science and Technology, University of Tokyo, Tokyo 113-8656, Japan. E-mail: kanno@mist.i.u-tokyo.ac.jp. Phone: +81-3-5841-6906. Fax: +81-3-5841-6886.

27, 33, 35, 45, 46, 55]. Particularly, recent attention has been attracted by, among others, but not limited to, level-set methods for continuum optimization [30, 32, 53, 54]. In this paper we examine applicability of an alternative framework, topology optimization of frame structures, in design of compliant mechanisms. Particular attention is focused on usage of standardized beam sections and direct treatment of the local stress constraints.

As is known well, design of compliant mechanisms inevitably involves two almost conflicting requirements [13, 44]: retaining flexibility to produce the kinematic performance and stiffness to ensure resistance against failure. To explore structures simultaneously fulfilling both requirements, in this paper we attempt to maximize the output displacement of a compliant mechanism under the local stress constraints. It is well known that the optimal solutions of continuum-based topology optimization approaches often have *de facto* hinges and, thence, stress concentration should be avoided by carrying out post-processing procedure [35]. As a remedy, hinge-free optimization methods have been studied extensively; e.g., methods imposing minimum length scale [36], adding two different sets of artificial springs [37], using wavelet parameterization [59], introducing a density filter [47], employing a quadratic energy function used in the filed of image processing [29], and performing multi-objective optimization of two differently defined measures of compliance [63]. Making use of topology optimization of frame structures might be able to be an alternative solution. Indeed, frame models are sometimes used in optimal design of compliant mechanisms [28, 34, 38, 42, 43]. This paper addresses local stress constraints and uses only standardized beam elements. The optimal solution has no hinge and consists of structural elements with straight shapes and a limited number of different cross-sections. This might be regarded as an advantage in manufacturability, as discussed below. Since the proposed method is based upon the ground structure method, a potential disadvantage is that the solution space is rather limited compared with continuum-based topology optimization.

This paper is inspired by the work of Jang *et al.* [22], in which design of compliant mechanisms was treated as a topology optimization problem of frame structures with an element-connectivity parameterization. Element-connectivity parameterization was originated by Yoon and Kim [58] as a design parameterization for continuum topology optimization; see [26, 52, 56, 57, 60, 61] for its developments. Jang *et al.* [22] applied the idea of the element-connectivity parameterization to frame structures. Namely, each member of a conventional ground structure is divided into three components: one center long beam, called a ground member, and two short beams, called joint elements, connected to both ends of the ground member. Then design variables are assigned only to the cross-sections of the joint elements; in essence, the bending stiffness of each joint element is considered a design variable. This parameterization is also employed in this paper. Small deformation is assumed throughout the paper.

In Jang *et al.* [22], the width of each joint element is treated as a continuous design variable. Then the maximization problem of the output displacement is solved with a nonlinear programming approach. A small positive lower bound is given to the width of a joint element in order to prevent numerical instability. After the optimization process, a joint element will be removed if its width is smaller than a certain threshold value. The method proposed in this paper is different from the one due to Jang *et al.* [22] in the following aspects.

(i) The cross-sections of both ground members and joint elements are standardized.

(ii) The optimization problem is formulated as a mixed-integer linear programming (MILP) problem. Therefore, algorithms with guaranteed convergence to a global optimal solution, e.g., a branch-and-cut method, are available.

(iii) The local stress constraints are considered.

(iv) The method does not require to use a small positive lower bound for the design variables. The static equilibrium equation is treated as constraints of the proposed MILP problem and numerical instability does not occur even if such a lower bound is not introduced.

(v) Various combinatorial constraints can be treated directly. Examples are prohibition of presence of mutually overlapping members and upper and lower bound constraints for the number of members connected to each node.

Regarding (i), the ground members can be standardized straightforwardly with the element-connectivity parameterization, because the cross-sections of ground members are fixed. Jang *et al.* [22] performed optimization of continuous design variables, which leads to the optimal solution with non-standardized joint elements. Compared with solutions of conventional continuum-based topology optimization, compliant mechanisms with standardized beam elements might have an advantage that they can be converted into products without resorting to post-processing of the computational results. Also, some authors argued that, from a practical point of view, direct optimization of frame structures is sometimes preferable to continuum-based topology optimization followed by interpretation of the results as frame structures [15]. Concerning (ii), the MILP formulation proposed in this paper can be viewed as a natural extension of the one for frame optimization in [25]. Similar MILP formulations for structural optimization were developed for continua with binary design variables [48, 50], trusses with discrete member cross-sectional areas [24, 39], and tensegrity structures [23]. In a topology optimization process, the stress constraints mentioned in (iii) should be imposed only on existing members. In other words, if the cross-sectional area of a member reaches zero, then the stress constraint on this member should be removed from the optimization problem [2, 7, 41]. This constraint is fully addressed by employing the MILP approach, the fundamental idea of which is originated from Stolpe and Svanberg [50]. Existing studies, with few exceptions, consider the local stress constraints in design optimization of compliant mechanisms, although general frameworks of treatment of stress constraints in continuum-based topology optimization were studied in, e.g., [3, 4, 10, 17, 18, 20]. For compliant mechanism design, Saxena and Ananthasuresh [44] employed the relaxation technique of the stress constraints, due to Cheng and Guo [7], and solved the resulting optimization problem with a sequential quadratic programming. Lu and Kota [28] and Zhou and Mandalad [62] used genetic algorithms to solve problems involving the local stress constraints. An advantage of the MILP approach to these meta-heuristics and a nonlinear programming approach is guaranteed convergence to a global optimal solution. When we consider constraint (iii), as is known well, it is not accepted to use a small positive lower bound for the design variables; see, e.g., [6]. Thus property (iv) becomes crucial. This issue is resolved, again, by employing the MILP approach. Property (v) stems from the fact that the proposed formulation uses a set of binary variables to represent structural design.

A potential disadvantage of the proposed method is that computational cost for solving an MILP problem may possibly increase drastically as the number of design variables increases. As a remedy,

we propose a local search which is applicable to large-scale problems. The method uses two different types of neighborhoods alternately. We solve the original MILP problem with adding a constraint such that the solution should exist within a given neighborhood of the incumbent solution. This additional constraint is written as some linear inequality constraints. Thus in the local search we solve MILP subproblems sequentially. Similar local searches based upon MILP were proposed for topology optimization of continua [49] and frame structures [25]. Use of integer programming in a local search has received increasing attention as one of heuristics for various optimization problems, including vehicle routing problems [9, 16], service network design problems [11], etc. General frameworks of such methods can be found in, e.g., [8, 12, 19].

The paper is organized as follows. Section 2 defines the design optimization problem for generating a compliant mechanism based upon the element-connectivity parameterization of a frame structure. Section 3 shows that this optimization problem can be reformulated as an MILP problem. In section 4 we propose a local search heuristic for solving large-scale problems. Section 5 presents numerical experiments. We conclude in section 6.

A few words regarding notation. All vectors are assumed to be column vectors. The $(m+n)$-dimensional column vector $(\boldsymbol{s}^\top, \boldsymbol{x}^\top)^\top$ consisting of $\boldsymbol{s} \in \mathbb{R}^m$ and $\boldsymbol{x} \in \mathbb{R}^n$ is often written simply as $(\boldsymbol{s}, \boldsymbol{x})$. The ℓ^1-norm of vector $\boldsymbol{x} = (x_1, \ldots, x_n)^\top \in \mathbb{R}^n$ is defined by

$$\|\boldsymbol{x}\|_1 = \sum_{i=1}^{n} |x_i|.$$

For set $\mathcal{S}$, we use $|\mathcal{S}|$ to denote its cardinality. For instance, if $\mathcal{S} = \{1, \ldots, m\}$, then $|\mathcal{S}| = m$.

2 Design of compliant mechanisms

Section 2.1 summarizes the concept of an extended ground structure due to Jang *et al.* [22]. Section 2.2 formulates a design optimization problem to generate a compliant mechanism that consists of beam elements with varying cross-sections.

2.1 Extended ground structure

Like a conventional ground structure approach to topology optimization of planar frame structures, we prepare a frame structure consisting of many candidate members and nodes with specified locations. An example is shown in Figure 1(a).

Following Jang *et al.* [22], each member is divided into three components: a center long beam, called a *ground member*, and two short beams, called *joint elements*, which are connected to both ends of the ground beam. Figure 1(b) shows the *extended ground structure* that is obtained in this manner. Let $\tilde{\mathcal{E}}$ and $\mathcal{E}^{\mathrm{J}}$ denote the set of ground members and the set of joint elements, respectively. For ground member $e \in \tilde{\mathcal{E}}$, we use $j_1(e)$ and $j_2(e)$ to denote the two joint elements that are connected to e. Ground members and joint elements are modeled as Timoshenko beam elements. As detailed in section 2.2, the dimensions of cross-sections of joint elements are treated as design variables in an optimization process.

We call a node connecting some joint elements a *ground node*. A node connecting a ground member and a joint element is called an *intermediate node*. It is worth noting that both ends of a

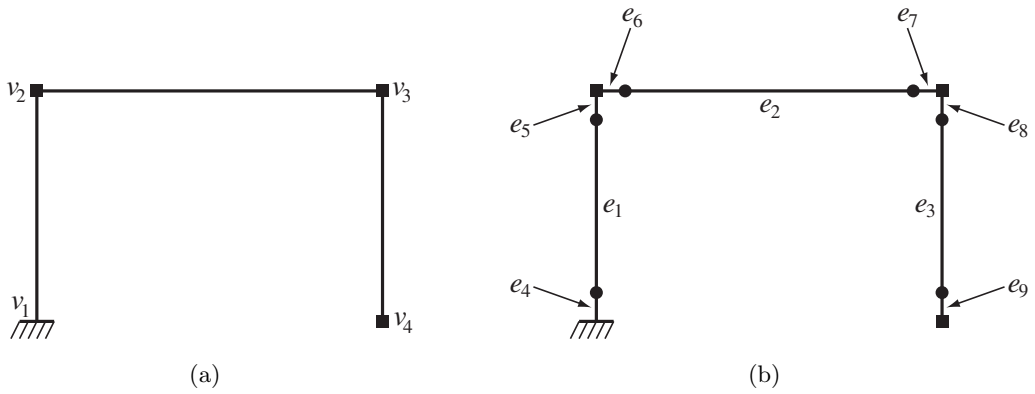

(a) (b)

Figure 1: An example of problem setting. (a) A design domain; and (b) the corresponding ground structure.

ground member are intermediate nodes. Let $\tilde{\mathcal{V}}$ denote the set of ground nodes. We use d to denote the number of degrees of freedom of displacements of the extended ground structure. It should be clear that d includes degrees of freedom of intermediate nodes.

Example 2.1. The ground structure shown in Figure 1(a) consists of three members connected to four nodes. Node v_1 is a fixed support. The corresponding extended ground structure is shown in Figure 1(b). The set of ground nodes is $\tilde{\mathcal{V}} = \{v_1, v_2, v_3, v_4\}$. Intermediate nodes are depicted as filled circles. Since the extended ground structure has 9 free nodes, the number of degrees of freedom of displacements is $d = 27$. The set of ground members is

$$\tilde{\mathcal{E}} = \{e_1, e_2, e_3\}.$$

Each ground member is connected to two joint elements as

$$\begin{aligned} j_1(e_1) &= e_4, \quad j_2(e_1) = e_5, \\ j_1(e_2) &= e_6, \quad j_2(e_2) = e_7, \\ j_1(e_3) &= e_8, \quad j_2(e_3) = e_9. \end{aligned}$$

The set of all joint elements is

$$\mathcal{E}^{\mathrm{J}} = \{e_4, e_5, e_6, e_7, e_8, e_9\}.$$

The cross-sections of these 6 joint elements are to be designed in the optimization process. ■

2.2 Design optimization problem

In the course of optimization, only dimensions of the cross-sections of the joint elements are considered design variables. Shapes of the ground members are fixed. Topology of the structure can change if some of joint elements vanish as a result of optimization. This is a key idea of the so-called element-connectivity parameterization method [22, 58].

In this paper, design variables are considered discrete. That is, section of each beam is chosen from a set of some given candidates. Selection of the beam sections is handled directly within the framework of integer programming. This is one of major differences from the method of [22],

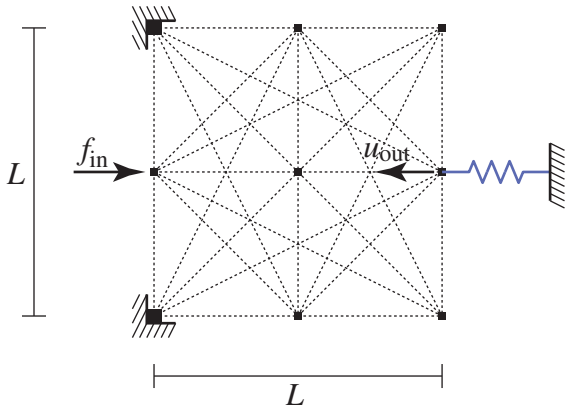

Figure 2: Problem setting for design of a compliant inverter. The ground structure, input force, output displacement, and output spring.

in which the width of each beam is treated as a continuous design variable and the optimization problem is attacked with a nonlinear programming approach using the sensitivity analysis.

Figure 2 shows an example of ground structure, with which we attempt to design a compliant force inverter. Ground nodes are depicted as filled squares, while intermediate nodes are omitted in Figure 2. Like existing studies on optimal design of compliant mechanisms, we consider the following design problem. The left node in the middle row, called the *input node*, of the structure is subjected to a specified (rightward) external force, denoted by f_{in}. The right node in the middle row, called the *output node*, is connected to an additional spring, called the *output spring*. The top and bottom leftmost nodes are fixed supports. Then we attempt to find the set of beam sections of joint elements that maximizes the horizontal (leftward) displacement of the output node, denoted by u_{out}.

For simplicity, we assume that all the ground members have the same section. In the optimization process, we determine whether joint element $j \in \mathcal{E}^{\text{J}}$ has

(i) the same section as the ground member;

(ii) the section with the predetermined small bending stiffness; or

(iii) no stiffness (i.e., joint element j is removed).

Let $\mathcal{J}_{\text{stiff}}$, $\mathcal{J}_{\text{flex}}$, and $\mathcal{N}$ denote the sets of joint elements in phases (i), (ii), and (iii), respectively. Figure 3 illustrates these three phases for joint element $j_1(e)$. As detailed in section 3.2, if $j_1(e) \in \mathcal{N}$, then ground member e can be considered to be removed. A joint element in $\mathcal{J}_{\text{stiff}}$ is considered to form a usual joint of a frame structure. In contrast, the one in $\mathcal{J}_{\text{flex}}$ gives rotational flexibility to the end of a ground member and serves as an elastic hinge. Removed joint elements, i.e., the ones belonging to $\mathcal{N}$, lead to change of structural topology.

In the setting above, the design problem can be regarded as a problem finding a partition

$$\mathcal{E}^{\text{J}} = \mathcal{J}_{\text{stiff}} \cup \mathcal{J}_{\text{flex}} \cup \mathcal{N} \tag{1}$$

of $\mathcal{E}^{\text{J}}$, where $\mathcal{J}_{\text{stiff}}$, $\mathcal{J}_{\text{flex}}$, and $\mathcal{N}$ are disjoint sets. For joint element $j \in \mathcal{E}^{\text{J}}$, let a_j and I_j denote the

Figure 3: Three phases of a joint element. (a) $j_1(e) \in \mathcal{J}_{\text{stiff}}$; (b) $j_1(e) \in \mathcal{J}_{\text{stiff}}$; and (c) $j_1(e) \in \mathcal{N}$.

member cross-sectional area and moment of inertia, respectively, which are given by

$$(a_j, I_j) = \begin{cases} (\bar{a}^{\text{s}}, \bar{I}^{\text{s}}) & \text{if } j \in \mathcal{J}_{\text{stiff}}, \\ (\bar{a}^{\text{f}}, \bar{I}^{\text{f}}) & \text{if } j \in \mathcal{J}_{\text{flex}}, \\ (0, 0) & \text{if } j \in \mathcal{N}. \end{cases} \tag{2}$$

Here, $\bar{a}^{\text{s}}$, $\bar{a}^{\text{f}}$, $\bar{I}^{\text{s}}$, and $\bar{I}^{\text{f}}$ are predetermined constants satisfying $\bar{a}^{\text{s}} \geq \bar{a}^{\text{f}} > 0$ and $\bar{I}^{\text{s}} \gg \bar{I}^{\text{f}} > 0$. For notational convenience, we use vectors $\boldsymbol{a} = (a_j \mid j \in \mathcal{E}^{\text{J}})$ and $\boldsymbol{I} = (I_j \mid j \in \mathcal{E}^{\text{J}})$.

Let $\boldsymbol{u} \in \mathbb{R}^d$ denote the vector of nodal displacements of the extended ground structure. We use $\boldsymbol{f} \in \mathbb{R}^d$ to denote the external force vector, where its component corresponding to the input force is equal to f_{in} and all the other components are 0. Assume small deformation. The displacement vector at the equilibrium state subjected to the input force is given by the equilibrium equation,

$$(K(\boldsymbol{a}, \boldsymbol{I}) + K_{\text{out}})\boldsymbol{u} = \boldsymbol{f}. \tag{3}$$

Here, $K(\boldsymbol{a}, \boldsymbol{I}) \in \mathbb{R}^{d \times d}$ and $K_{\text{out}} \in \mathbb{R}^{d \times d}$ are the stiffness matrices of the extended ground structure and the output spring, respectively. Note that K_{out} is a constant matrix, because the elongation stiffness of the output spring is fixed. The explicit form of $K(\boldsymbol{a}, \boldsymbol{I})$ appears in section 3.1.

Noting that external forces are not applied to the intermediate nodes, we formulate the stress constraints only for joint elements as follows. Let v_1 and v_2 denote the two nodes of joint element j, i.e., $j = (v_1, v_2) \in \mathcal{E}^{\text{J}}$. Suppose that joint element j has the same section as the ground members, i.e., $j \in \mathcal{J}_{\text{stiff}}$. Let q^{s}_{y} and m^{s}_{y} denote the specified allowable (absolute) values of the axial force and the end moment, respectively. Define $\varphi^{\text{s}}_j : \mathbb{R}^d \to \mathbb{R}$ by

$$\varphi^{\text{s}}_j(\boldsymbol{u}) = \frac{|q^{\text{s}}_j(\boldsymbol{u})|}{q^{\text{s}}_{\text{y}}} + \frac{\max\{|m^{\text{s}}_{j,v_1}(\boldsymbol{u})|, |m^{\text{s}}_{j,v_2}(\boldsymbol{u})|\}}{m^{\text{s}}_{\text{y}}} - 1, \tag{4}$$

where $q^{\text{s}}_j(\boldsymbol{u})$ is the axial force and $m^{\text{s}}_{j,v_1}(\boldsymbol{u})$ and $m^{\text{s}}_{j,v_2}(\boldsymbol{u})$ are the two end moments induced by displacement $\boldsymbol{u}$. Then the stress constraint for joint element j is given by $\varphi^{\text{s}}_j(\boldsymbol{u}) \leq 0$. Similarly, if joint element j has small bending stiffness, i.e., $j \in \mathcal{J}_{\text{stiff}}$, then the stress constraint is written as $\varphi^{\text{f}}_j(\boldsymbol{u}) \leq 0$ with function $\varphi^{\text{f}}_j : \mathbb{R}^d \to \mathbb{R}$ defined by

$$\varphi^{\text{f}}_j(\boldsymbol{u}) = \frac{|q^{\text{f}}_j(\boldsymbol{u})|}{q^{\text{f}}_{\text{y}}} + \frac{\max\{|m^{\text{f}}_{j,v_1}(\boldsymbol{u})|, |m^{\text{f}}_{j,v_2}(\boldsymbol{u})|\}}{m^{\text{f}}_{\text{y}}} - 1. \tag{5}$$

Under all the constraints above, the design problem that we solve is to find a partition $\{\mathcal{J}_{\text{stiff}}, \mathcal{J}_{\text{flex}}, \mathcal{N}\}$

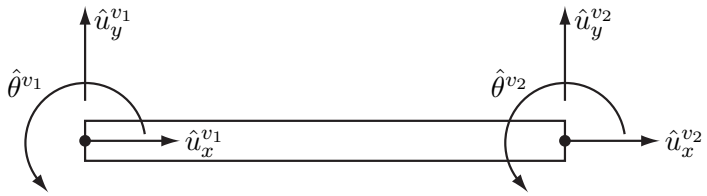

Figure 4: Local coordinate system for a joint element.

of $\mathcal{E}^{\mathrm{J}}$ that maximizes u_{out}. This optimization problem is formally written as

$$\begin{aligned}
&\max \quad && u_{\mathrm{out}} && && \text{(6a)}\\
&\text{s.t.} \quad && (K(\boldsymbol{a},\boldsymbol{I})+K_{\mathrm{out}})\boldsymbol{u}=\boldsymbol{f}, && && \text{(6b)}\\
& && \varphi_j^{\mathrm{s}}(\boldsymbol{u})\le 0, && \forall j\in\mathcal{J}_{\mathrm{stiff}}, && \text{(6c)}\\
& && \varphi_j^{\mathrm{f}}(\boldsymbol{u})\le 0, && \forall j\in\mathcal{J}_{\mathrm{flex}}, && \text{(6d)}\\
& && (a_j,I_j)=\begin{cases}(\bar{a}^{\mathrm{s}},\bar{I}^{\mathrm{s}}) & \text{if } j\in\mathcal{J}_{\mathrm{stiff}},\\ (\bar{a}^{\mathrm{f}},\bar{I}^{\mathrm{f}}) & \text{if } j\in\mathcal{J}_{\mathrm{flex}},\\ (0,0) & \text{if } j\notin\mathcal{J}_{\mathrm{stiff}}\cup\mathcal{J}_{\mathrm{flex}},\end{cases} && \forall j\in\mathcal{E}^{\mathrm{J}}, && \text{(6e)}
\end{aligned}$$

where $\mathcal{J}_{\mathrm{stiff}}$ and $\mathcal{J}_{\mathrm{flex}}$ are disjoint subsets of $\mathcal{E}^{\mathrm{J}}$. It should be clear here that variable u_{out} is a component of vector $\boldsymbol{u}$.

Remark 2.2. In the preceding study of Jang *et al.* [22], the upper bound constraint for the structural volume is (approximately) considered. This constraint is often considered also in continuum optimization approaches to design of compliant mechanisms; see, e.g., [33, 35, 45, 46]. Contrary to the compliance minimization, however, increase of the available structural volume does not necessarily imply improvement of performance of a compliant mechanism, as mentioned in [22]. For this reason, the volume constraint is not incorporated into problem (6). If necessary, however, the method developed in this paper can deal with the volume constraint easily; see Remark 3.1 in section 3.4. ■

3 Mixed-integer programming approach

Section 2 has defined a design optimization problem of a compliant mechanism as frame optimization with an extended ground structure. This section shows that the optimization problem, (6), can be reduced to an MILP problem. This MILP formulation can be viewed as a natural extension of the one due to Kureta and Kanno [25], which deals with frame optimization with a conventional ground structure. In the following, some details of the reformulation techniques in [25] are modified so as to match particular features of the formulation with an extended ground structure.

3.1 Equilibrium equations with element-connectivity formulation

This section develops an explicit formulation of the equilibrium equation, (6b), in conjunction with selection of beam sections, (6e). A key to this reformulation is diagonalization of the stiffness matrix, which was used also in [25].

For joint element $j\in\mathcal{E}^{\mathrm{J}}$, let v_1 and v_2 denote the two end nodes, i.e., $j=(v_1,v_2)$. We use $\hat{\boldsymbol{u}}_j=(\hat{u}_x^{v_1},\hat{u}_y^{v_1},\hat{\theta}^{v_1},\hat{u}_x^{v_2},\hat{u}_y^{v_2},\hat{\theta}^{v_2})^\top\in\mathbb{R}^6$ to denote the element displacement vector defined in the

local coordinate system as illustrated in Figure 4. We may decompose $\hat{\boldsymbol{u}}_j$ into three components of rigid-body motion and three components of deformation. We use $c_{j,1}$, $c_{j,2}$, $c_{j,3} \in \mathbb{R}$ to denote the generalized strains that describe this deformation. The compatibility relations between $c_{j,t}$ $(t = 1, 2, 3)$ and $\hat{\boldsymbol{u}}_j$ can be written as

$$c_{j,t} = \hat{\boldsymbol{b}}_{j,t}^{\top} \hat{\boldsymbol{u}}_j, \quad t = 1, 2, 3. \tag{7}$$

Constant vectors $\hat{\boldsymbol{b}}_{j,1}$, $\hat{\boldsymbol{b}}_{j,2}$, $\hat{\boldsymbol{b}}_{j,3} \in \mathbb{R}^6$ are defined by

$$\hat{\boldsymbol{b}}_{j,1} = \begin{bmatrix} -1 \\ 0 \\ 0 \\ 1 \\ 0 \\ 0 \end{bmatrix}, \quad \hat{\boldsymbol{b}}_{j,2} = \begin{bmatrix} 0 \\ 2/l_j \\ 1 \\ 0 \\ -2/l_j \\ 1 \end{bmatrix}, \quad \hat{\boldsymbol{b}}_{j,3} = \begin{bmatrix} 0 \\ 0 \\ -1 \\ 0 \\ 0 \\ 1 \end{bmatrix}, \tag{8}$$

where l_j is the length of joint element j. The displacement vector of the whole extended ground structure, $\boldsymbol{u} \in \mathbb{R}^d$, is defined with respect to the global coordinate system. Transformation of $\boldsymbol{u}$ to $\hat{\boldsymbol{u}}_j$ is written as

$$\hat{\boldsymbol{u}}_j = T_j \boldsymbol{u}, \tag{9}$$

where $T_j \in \mathbb{R}^{6 \times d}$ is a constant matrix. Define $\boldsymbol{b}_{j,1}$, $\boldsymbol{b}_{j,2}$, $\boldsymbol{b}_{j,3} \in \mathbb{R}^d$ by

$$\boldsymbol{b}_{j,t} = T_j^{\top} \hat{\boldsymbol{b}}_{j,t}, \quad t = 1, 2, 3. \tag{10}$$

From (7), (9), and (10), the compatibility relations between $c_{j,t}$ $(t = 1, 2, 3)$ and $\boldsymbol{u}$ are given by

$$c_{j,t} = \boldsymbol{b}_{j,t}^{\top} \boldsymbol{u}, \quad t = 1, 2, 3. \tag{11}$$

Similarly, for ground member $e \in \tilde{\mathcal{E}}$, the compatibility relations are written as

$$\tilde{c}_{e,t} = \tilde{\boldsymbol{b}}_{e,t}^{\top} \boldsymbol{u}, \quad t = 1, 2, 3, \tag{12}$$

where $\tilde{c}_{e,1}$, $\tilde{c}_{e,2}$, $\tilde{c}_{e,3} \in \mathbb{R}$ are the generalized strains and $\tilde{\boldsymbol{b}}_{e,1}$, $\tilde{\boldsymbol{b}}_{e,2}$, $\tilde{\boldsymbol{b}}_{e,3} \in \mathbb{R}^d$ are constant vectors.

In accordance with (11) and (12), the force-balance equation is written as

$$\sum_{j \in \mathcal{E}^{\mathrm{J}}} \sum_{t=1}^{3} s_{j,t} \boldsymbol{b}_{j,t} + \sum_{e \in \tilde{\mathcal{E}}} \sum_{t=1}^{3} \tilde{s}_{e,t} \tilde{\boldsymbol{b}}_{e,t} + K_{\mathrm{out}} \boldsymbol{u} = \boldsymbol{f}. \tag{13}$$

Here, for joint element $j \in \mathcal{E}^{\mathrm{J}}$, variables $s_{j,1}$, $s_{j,2}$, $s_{j,3} \in \mathbb{R}$ are the generalized stresses that are work-conjugate to $c_{j,1}$, $c_{j,2}$, and $c_{j,3}$. Similarly, $\tilde{s}_{e,1}$, $\tilde{s}_{e,2}$, $\tilde{s}_{e,3} \in \mathbb{R}$ are the generalized stresses of ground member $e \in \tilde{\mathcal{E}}$.

The constitutive laws are written as

$$s_{j,t} = k_{j,t} c_{j,t}, \quad t = 1, 2, 3; \ \forall e \in \mathcal{E}^{\mathrm{J}}, \tag{14}$$

$$\tilde{s}_{e,t} = \tilde{k}_{e,t} \tilde{c}_{e,t}, \quad t = 1, 2, 3; \ \forall j \in \tilde{\mathcal{E}}. \tag{15}$$

The member stiffnesses, $k_{j,t}$ $(t = 1, 2, 3)$, of joint element j depends on its phase as

$$k_{j,t} = \begin{cases} k^{\mathrm{s}}_{j,t} & \text{if } j \in \mathcal{J}_{\mathrm{stiff}}, \\ k^{\mathrm{f}}_{j,t} & \text{if } j \in \mathcal{J}_{\mathrm{flex}}, \\ 0 & \text{if } j \in \mathcal{N}, \end{cases} \qquad t = 1, 2, 3;\ \forall e \in \mathcal{E}^{\mathrm{J}}, \tag{16}$$

where $k^{\mathrm{s}}_{j,t}$ and $k^{\mathrm{f}}_{j,t}$ $(t = 1, 2, 3)$ are constants defined by

$$k^{\mathrm{s}}_{j,1} = \frac{E\bar{a}^{\mathrm{s}}}{l_j}, \quad k^{\mathrm{s}}_{j,2} = l_j\Big(\frac{l_j^2}{3E\bar{I}^{\mathrm{s}}} + \frac{4}{\kappa G\bar{a}^{\mathrm{s}}}\Big)^{-1}, \quad k^{\mathrm{s}}_{j,3} = \frac{E\bar{I}^{\mathrm{s}}}{l_j}, \tag{17a}$$

$$k^{\mathrm{f}}_{j,1} = \frac{E\bar{a}^{\mathrm{f}}}{l_j}, \quad k^{\mathrm{f}}_{j,2} = l_j\Big(\frac{l_j^2}{3E\bar{I}^{\mathrm{f}}} + \frac{4}{\kappa G\bar{a}^{\mathrm{f}}}\Big)^{-1}, \quad k^{\mathrm{f}}_{j,3} = \frac{E\bar{I}^{\mathrm{f}}}{l_j}. \tag{17b}$$

Here, we adopt the MacNeal element [31, 40] in the Timoshenko beam theory, κ is the shear correction factor, and E and G are Young's modulus and the shear modulus of the material, respectively. Also, $\tilde{k}_{e,1}$, $\tilde{k}_{e,2}$, $\tilde{k}_{e,3} \in \mathbb{R}$ $(\forall e \in \tilde{\mathcal{E}})$ in (15) are constants which are defined for ground member e in a similar manner.

The upshot is that the equilibrium equation (6b), in conjunction with (6e), is equivalently rewritten as (11), (12), (13), (14), (15), and (16).

3.2 Constitutive laws with binary variables

Among the equations presented in section 3.1, (14) is a system of nonlinear constraints because $k_{j,t}$ is a variable determined by (16). This section rewrites these nonlinear constraints as some linear constraints by making use of some binary variables.

In the optimization process, section of each joint element is treated as a design variable and the set of joint elements is partitioned as (1). We begin by introducing binary variables to express this partition. Specifically, for joint element $j \in \mathcal{E}^{\mathrm{J}}$, we prepare two 0-1 variables,

$$(x_j, y_j) \in \{0, 1\}^2, \tag{18}$$

that satisfy

$$x_j + y_j \leq 1. \tag{19}$$

The partition of the set of joint elements in (1) can be expressed as

$$(x_j, y_j) = (1, 0) \quad \Leftrightarrow \quad j \in \mathcal{J}_{\mathrm{stiff}}, \tag{20a}$$

$$(x_j, y_j) = (0, 1) \quad \Leftrightarrow \quad j \in \mathcal{J}_{\mathrm{flex}}, \tag{20b}$$

$$(x_j, y_j) = (0, 0) \quad \Leftrightarrow \quad j \in \mathcal{N}. \tag{20c}$$

The constitutive laws of joint elements are given by (14) and (16). Variable $k_{j,t}$ can be eliminated as follows. For each $t = 1, 2, 3$ and $j \in \mathcal{E}^{\mathrm{J}}$, we decompose the generalized stress, $s_{j,t}$, additively into two parts as

$$s_{j,t} = s^{\mathrm{s}}_{j,t} + s^{\mathrm{f}}_{j,t}, \tag{21}$$

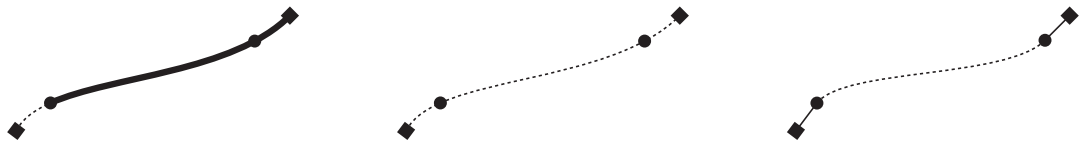

(a) (b) (c)

Figure 5: Three equivalent treatments of member e satisfying $(x_{j_1(e)}, y_{j_1(e)}) = (0,0)$ and $(x_{j_2(e)}, y_{j_2(e)}) = (1,0)$. (a) Joint element $j_1(e)$ has a vanished cross-section; (b) the ground member and the two joint elements have vanished cross-sections; and (c) the ground member has a vanished cross-section, while the two joint elements undergo no deformations.

where $s^{\mathrm{s}}_{j,t}$ and $s^{\mathrm{f}}_{j,t}$ are defined by

$$s^{\mathrm{s}}_{j,t} = \begin{cases} k^{\mathrm{s}}_{j,t} c_{j,t} & \text{if } j \in \mathcal{J}_{\mathrm{stiff}}, \\ 0 & \text{otherwise}, \end{cases} \qquad s^{\mathrm{f}}_{j,t} = \begin{cases} k^{\mathrm{f}}_{j,t} c_{j,t} & \text{if } j \in \mathcal{J}_{\mathrm{flex}}, \\ 0 & \text{otherwise}. \end{cases} \tag{22}$$

Then $s_{j,t}$ satisfies (14) and (16) if and only if $s_{j,t}$, $s^{\mathrm{s}}_{j,t}$, and $s^{\mathrm{f}}_{j,t}$ satisfy (21) and (22). With reference to (20), we can rewrite (22) equivalently by using the binary variables as

$$s^{\mathrm{s}}_{j,t} = k^{\mathrm{s}}_{j,t} c^{\mathrm{s}}_{j,t}, \qquad s^{\mathrm{f}}_{j,t} = k^{\mathrm{f}}_{j,t} c^{\mathrm{f}}_{j,t}, \tag{23}$$

$$c^{\mathrm{s}}_{j,t} = \begin{cases} c_{j,t} & \text{if } x_j = 1, \\ 0 & \text{if } x_j = 0, \end{cases} \qquad c^{\mathrm{f}}_{j,t} = \begin{cases} c_{j,t} & \text{if } y_j = 1, \\ 0 & \text{if } y_j = 0, \end{cases} \tag{24}$$

where $c^{\mathrm{s}}_{j,t}$ and $c^{\mathrm{f}}_{j,t}$ are additional variables.

We next introduce the notion of existence/nonexistence of a ground member. Originally, in [22], only the dimension (specifically, the width) of cross-section of each joint element is varied during the optimization process and no design variables are assigned to ground members. In contrast, in our approach it is more convenient to make use of design variables that explicitly represent the existence of ground members. For ground member $e \in \tilde{\mathcal{E}}$, let $z_e \in \{0,1\}$ be a variable such that $z_e = 1$ means the presence of member e and $z_e = 0$ means the absence of member e. Recall that we use $j_1(e)$ and $j_2(e)$ to denote the joint elements connected to ground member e. Suppose that at least one of the two joint elements has no stiffness. Figure 5(a) shows an example of $j_1(e) \in \mathcal{N}$ and $j_2(e) \in \mathcal{J}_{\mathrm{stiff}}$, i.e., $j_1(e)$ vanishes and $j_2(e) \in \mathcal{J}_{\mathrm{stiff}}$ has the same section as the ground members. Then the generalized stresses of $j_1(e)$ are equal to zero. Since ground member e is connected only to $j_1(e)$ and $j_2(e)$ through two intermediate nodes, the force-balance equation, (13), requires that the

Table 1: Member phases and integer variables.

	$(x_{j_1(e)}, y_{j_1(e)})$	$(x_{j_2(e)}, y_{j_2(e)})$	z_e
Case 1	$(1,0)$	$(1,0)$	1
Case 2	$(0,1)$	$(1,0)$	1
Case 3	$(1,0)$	$(0,1)$	1
Case 4	$(0,1)$	$(0,1)$	1
Case 5	$(0,0)$	$(0,0)$	0

generalized stresses of e and $j_2(e)$ are also equal to zero. This means that if $j_1(e)$ vanishes, then we can remove e and $j_2(e)$ without changing the equilibrium state of the whole structure. That is, the situation illustrated in Figure 5(a) can be replaced by the one in Figure 5(b). In this situation we may suppose that the displacements of the two intermediate nodes are allowed to take any values, in the sense that the displacements of the ground nodes remain unchanged. Thus, if at least one of $j_1(e)$, $j_2(e)$, and e vanishes, then all of these three members can be considered removed. In other words, we may require that $z_e = 1$ implies $(x_{j_1(e)}, y_{j_1(e)}) \neq (0,0)$ and $(x_{j_2(e)}, y_{j_2(e)}) \neq (0,0)$, and vice versa. This condition can be written as

$$z_e = x_{j_1(e)} + y_{j_1(e)} = x_{j_2(e)} + y_{j_2(e)}, \quad \forall e \in \tilde{\mathcal{E}}. \tag{25}$$

As a consequence, a ground member and its two adjacent joint elements can take one of the five cases listed in Table 1.

Consider the situation in which ground member $e \in \tilde{\mathcal{E}}$ vanishes, i.e., $z_e = 0$. The generalized stresses satisfy $\tilde{s}_{e,t} = 0$ $(t = 1,2,3)$. Then (15) implies $\tilde{c}_{e,t} = 0$ $(t = 1,2,3)$. From this observation it follows that we can replace (12) by

$$\tilde{c}_{e,t} = \begin{cases} \tilde{\boldsymbol{b}}_{e,t}^{\top} \boldsymbol{u} & \text{if } z_e = 1, \\ 0 & \text{if } z_e = 0, \end{cases} \tag{26}$$

without changing the solution.[1] Furthermore, from (25) we see that $z_e = 0$ holds only if the two adjacent joint elements vanish. Since ground member e is connected only to these two joint elements, the force-balance equation, (13), requires $\tilde{s}_{e,t} = 0$ (and, thence, $\tilde{c}_{e,t} = 0$ from (15)) when the two adjacent joint elements vanish. In short, if $z_e = 0$, then $\tilde{c}_{e,t} = 0$ holds from the force-balance equation. Hence, we can replace (26) by

$$|\tilde{c}_{e,t} - \tilde{\boldsymbol{b}}_{e,t}^{\top} \boldsymbol{u}| \leq M(1 - z_e), \tag{27}$$

where $M \gg 0$ is a sufficiently large constant.

We further analyze the constitutive law of joint element $j \in \mathcal{E}^{\mathrm{J}}$. Recall that the constitutive law of the joint element has been given by (21), (23), and (24). When joint element j vanishes, i.e., $(x_j, y_j) = (0,0)$, we suppose that the adjacent ground member also vanishes, as illustrated in Figure 5(b). In this situation, suppose that the two joint elements are required to undergo no deformations, as illustrated in Figure 5(c). Even if under this artificial constraint, the equilibrium state of the whole structure does not change; more precisely, the displacements of the ground nodes at the equilibrium state remain unchanged. From this observation it follows that the condition

$$c_{j,t} = 0 \quad \text{if } (x_j, y_j) = (0,0) \tag{28}$$

can be added to the constitutive law of the joint element. Conditions (24) and (28) can be rewritten equivalently by using the binary variables as

$$|c_{j,t}^{\mathrm{s}}| \leq M x_j, \tag{29a}$$

$$|c_{j,t}^{\mathrm{f}}| \leq M y_j, \tag{29b}$$

$$c_{j,t}^{\mathrm{s}} + c_{j,t}^{\mathrm{f}} = c_{j,t}, \tag{29c}$$

[1] Here, $z_e = 0$ does not imply $\tilde{\boldsymbol{b}}_{e,t}^{\top} \boldsymbol{u} = 0$.

where $M \gg 0$ is a sufficiently large constant. In (29), variable $c_{j,t}$ can be eliminated by using (11).

By summing up the results above, we can see that the constitutive law of a joint element is rewritten as (21), (23), and (29), where the binary variables satisfy (18), (19), and (25). Also, the constitutive law, in conjunction with the compatibility relation, of a ground member is written as (15) and (27).

3.3 On stress constraints

In this section we show that (29a) and (29b) can be replaced by local stress constraints.

Recall that variables $c^{\mathrm{s}}_{j,t}$ and $c^{\mathrm{f}}_{j,t}$ in (29) have been related to $s^{\mathrm{s}}_{j,t}$ and $s^{\mathrm{f}}_{j,t}$ through (23). Since $k^{\mathrm{s}}_{j,t}$ and $k^{\mathrm{f}}_{j,t}$ are positive constants and M is sufficiently large, (29a) and (29b) (for all t and j) can be replaced by

$$|s^{\mathrm{s}}_{j,t}| \le M x_j, \quad t = 1,2,3;\ \forall j \in \mathcal{E}^{\mathrm{J}}, \tag{30}$$

$$|s^{\mathrm{f}}_{j,t}| \le M y_j, \quad t = 1,2,3;\ \forall j \in \mathcal{E}^{\mathrm{J}}. \tag{31}$$

On the other hand, for joint elements belonging to $\mathcal{J}_{\mathrm{stiff}}$, the stress constraints have been given by (6c) in conjunction with (4). Let $\bar{\sigma}$ denote the specified upper bound for stress. We use $\bar{Z}^{\mathrm{s}}$ to denote the elastic section modulus of the cross-section used for $j \in \mathcal{J}_{\mathrm{stiff}}$. Then $q^{\mathrm{s}}_{\mathrm{y}}$ and $m^{\mathrm{s}}_{\mathrm{y}}$ in (4) are written as $q^{\mathrm{s}}_{\mathrm{y}} = \bar{\sigma}\bar{a}^{\mathrm{s}}$ and $m^{\mathrm{s}}_{\mathrm{y}} = \bar{\sigma}\bar{Z}^{\mathrm{s}}$. Hence, the stress constraints for $j \in \mathcal{J}_{\mathrm{stiff}}$, (6c), can be rewritten as

$$\frac{|q^{\mathrm{s}}_j(\boldsymbol{u})|}{\bar{a}^{\mathrm{s}}} + \frac{\max\{|m^{\mathrm{s}}_{j,v_1}(\boldsymbol{u})|, |m^{\mathrm{s}}_{j,v_2}(\boldsymbol{u})|\}}{\bar{Z}^{\mathrm{s}}} \le \bar{\sigma}, \quad \forall j \in \mathcal{J}_{\mathrm{stiff}}. \tag{32}$$

From the definition of $\boldsymbol{b}_{j,t}$, i.e., (8) and (10), we obtain

$$s^{\mathrm{s}}_{j,1} = q^{\mathrm{s}}_j(\boldsymbol{u}), \quad s^{\mathrm{s}}_{j,2} = \frac{m^{\mathrm{s}}_{j,v_1}(\boldsymbol{u}) + m^{\mathrm{s}}_{j,v_2}(\boldsymbol{u})}{2}, \quad s^{\mathrm{s}}_{j,3} = \frac{-m^{\mathrm{s}}_{j,v_1}(\boldsymbol{u}) + m^{\mathrm{s}}_{j,v_2}(\boldsymbol{u})}{2}.$$

Therefore, the left-hand side of (32) can be reduced to

$$\begin{aligned}
&\frac{|q^{\mathrm{s}}_j(\boldsymbol{u})|}{\bar{a}^{\mathrm{s}}} + \frac{\max\{|m^{\mathrm{s}}_{j,v_1}(\boldsymbol{u})|, |m^{\mathrm{s}}_{j,v_2}(\boldsymbol{u})|\}}{\bar{Z}^{\mathrm{s}}} \\
&\quad = \frac{|q^{\mathrm{s}}_j(\boldsymbol{u})|}{\bar{a}^{\mathrm{s}}} + \frac{1}{2}\frac{|m^{\mathrm{s}}_{j,v_1}(\boldsymbol{u}) + m^{\mathrm{s}}_{j,v_2}(\boldsymbol{u})|}{\bar{Z}^{\mathrm{s}}} + \frac{1}{2}\frac{|m^{\mathrm{s}}_{j,v_1}(\boldsymbol{u}) - m^{\mathrm{s}}_{j,v_2}(\boldsymbol{u})|}{\bar{Z}^{\mathrm{s}}} \\
&\quad = \frac{|s^{\mathrm{s}}_{j,1}|}{\bar{a}^{\mathrm{s}}} + \frac{|s^{\mathrm{s}}_{j,2}|}{\bar{Z}^{\mathrm{s}}} + \frac{|s^{\mathrm{s}}_{j,3}|}{\bar{Z}^{\mathrm{s}}}.
\end{aligned}$$

Consequently, (32) is equivalently rewritten as

$$\frac{|s^{\mathrm{s}}_{j,1}|}{\bar{a}^{\mathrm{s}}} + \frac{|s^{\mathrm{s}}_{j,2}|}{\bar{Z}^{\mathrm{s}}} + \frac{|s^{\mathrm{s}}_{j,3}|}{\bar{Z}^{\mathrm{s}}} \le \bar{\sigma}, \quad \forall j \in \mathcal{J}_{\mathrm{stiff}}. \tag{33}$$

Similarly, the stress constraint for joint elements belonging to $\mathcal{J}_{\mathrm{flex}}$, i.e., (6d) with (5), can be rewritten equivalently as

$$\frac{|s^{\mathrm{f}}_{j,1}|}{\bar{a}^{\mathrm{f}}} + \frac{|s^{\mathrm{f}}_{j,2}|}{\bar{Z}^{\mathrm{f}}} + \frac{|s^{\mathrm{f}}_{j,3}|}{\bar{Z}^{\mathrm{f}}} \le \bar{\sigma}, \quad \forall j \in \mathcal{J}_{\mathrm{flex}}. \tag{34}$$

Finally, we can see that (30) and (33) are equivalent to

$$\frac{|s^{\mathrm{s}}_{j,1}|}{\bar{a}^{\mathrm{s}}} + \frac{|s^{\mathrm{s}}_{j,2}|}{\bar{Z}^{\mathrm{s}}} + \frac{|s^{\mathrm{s}}_{j,3}|}{\bar{Z}^{\mathrm{s}}} \le \bar{\sigma} x_j, \quad \forall j \in \mathcal{E}^{\mathrm{J}}. \tag{35}$$

Also, (31) and (34) are equivalent to

$$\frac{|s^{\mathrm{f}}_{j,1}|}{\bar{a}^{\mathrm{f}}} + \frac{|s^{\mathrm{f}}_{j,2}|}{\bar{Z}^{\mathrm{f}}} + \frac{|s^{\mathrm{f}}_{j,3}|}{\bar{Z}^{\mathrm{f}}} \leq \bar{\sigma} y_j, \quad \forall j \in \mathcal{E}^{\mathrm{J}}. \tag{36}$$

In this way, constraints (29a) and (29b) can be replaced by constraints (35) and (36).

3.4 Mixed-integer linear programming formulation

By summing up the results obtained in the preceding sections, we are now in position to present an MILP problem that we solve. The constraints of problem (6) can be expressed as (11), (13), (15), (19), (21), (23), (25), (27), (29c), (35), and (36). Therefore, problem (6) is reduced to the following MILP problem:

$$\begin{aligned}
\max \quad & u_{\mathrm{out}} && && \text{(37a)}\\
\text{s.t.} \quad & \sum_{e\in\tilde{\mathcal{E}}}\sum_{t=1}^{3} \tilde{s}_{e,t}\tilde{\boldsymbol{b}}_{e,t} + \sum_{j\in\mathcal{E}^{\mathrm{J}}}\sum_{t=1}^{3}(s^{\mathrm{s}}_{j,t}+s^{\mathrm{f}}_{j,t})\boldsymbol{b}_{j,t} + K_{\mathrm{out}}\boldsymbol{u} = \boldsymbol{f}, && && \text{(37b)}\\
& \frac{|s^{\mathrm{s}}_{j,1}|}{\bar{a}^{\mathrm{s}}} + \frac{|s^{\mathrm{s}}_{j,2}|}{\bar{Z}^{\mathrm{s}}} + \frac{|s^{\mathrm{s}}_{j,3}|}{\bar{Z}^{\mathrm{s}}} \leq \bar{\sigma} x_j, && \forall j \in \mathcal{E}^{\mathrm{J}}, && \text{(37c)}\\
& \frac{|s^{\mathrm{f}}_{j,1}|}{\bar{a}^{\mathrm{f}}} + \frac{|s^{\mathrm{f}}_{j,2}|}{\bar{Z}^{\mathrm{f}}} + \frac{|s^{\mathrm{f}}_{j,3}|}{\bar{Z}^{\mathrm{f}}} \leq \bar{\sigma} y_j, && \forall j \in \mathcal{E}^{\mathrm{J}}, && \text{(37d)}\\
& s^{\mathrm{s}}_{j,t} = k^{\mathrm{s}}_{j,t} c^{\mathrm{s}}_{j,t}, \quad s^{\mathrm{f}}_{j,t} = k^{\mathrm{f}}_{j,t} c^{\mathrm{f}}_{j,t}, && t=1,2,3;\ \forall j \in \mathcal{E}^{\mathrm{J}}, && \text{(37e)}\\
& \tilde{s}_{e,t} = \tilde{k}_{e,t}\tilde{c}_{e,t} && t=1,2,3;\ \forall e \in \tilde{\mathcal{E}}, && \text{(37f)}\\
& c^{\mathrm{s}}_{j,t} + c^{\mathrm{f}}_{j,t} = \boldsymbol{b}^{\top}_{j,t}\boldsymbol{u}, && t=1,2,3;\ \forall j \in \mathcal{E}^{\mathrm{J}}, && \text{(37g)}\\
& |\tilde{c}_{e,t} - \tilde{\boldsymbol{b}}^{\top}_{e,t}\boldsymbol{u}| \leq M(1-z_e), && t=1,2,3;\ \forall e \in \tilde{\mathcal{E}}, && \text{(37h)}\\
& z_e = x_{j_1(e)} + y_{j_1(e)} = x_{j_2(e)} + y_{j_2(e)}, && \forall e \in \tilde{\mathcal{E}}, && \text{(37i)}\\
& x_j + y_j \leq 1, && \forall j \in \mathcal{E}^{\mathrm{J}}, && \text{(37j)}\\
& x_j, y_j \in \{0,1\}, && \forall j \in \mathcal{E}^{\mathrm{J}}, && \text{(37k)}\\
& z_e \in \{0,1\}, && \forall e \in \tilde{\mathcal{E}}. && \text{(37l)}
\end{aligned}$$

In problem (37), continuous variables are $s^{\mathrm{s}}_{j,t}$, $s^{\mathrm{f}}_{j,t}$, $c^{\mathrm{s}}_{j,t}$, $c^{\mathrm{f}}_{j,t}$ (for all j and t), $\tilde{s}_{e,t}$, $\tilde{c}_{e,t}$ (for all e and t), and $\boldsymbol{u}$. Binary variables are x_j, y_j (for all j) and z_e (for all e). Note that constraint (37l) is redundant, because (37i), (37j), and (37k) imply (37l). All the constraints other than (37k) and (37l) are linear constraints. Thus problem (37) is an MILP problem and, hence, can be solved globally with an existing algorithm, e.g., a branch-and-cut method. Several software packages, e.g., SCIP [1] and CPLEX [21], are available for this purpose.

The remainder of the section is devoted to exploring some additional constraints that can be handled within the framework of MILP.

We begin with the constraints that prohibit presence of mutually intersecting members lying in the same plane. Let $\tilde{\mathcal{P}}_{\mathrm{cross}}$ denote the set of pairs of ground members that mutually intersect in the ground structure. That is, we write $(e, e') \in \tilde{P}_{\mathrm{cross}}$ if member $e \in \tilde{\mathcal{E}}$ and member $e' \in \tilde{\mathcal{E}}$ intersect. Recall that $z_e = 1$ means presence of member e, while $z_e = 0$ means absence of member e. Therefore, z_e and $z_{e'}$ cannot become 1 simultaneously. This condition can be written as

$$z_e + z_{e'} \leq 1, \quad \forall (e, e') \in \tilde{\mathcal{P}}_{\mathrm{cross}}. \tag{38}$$

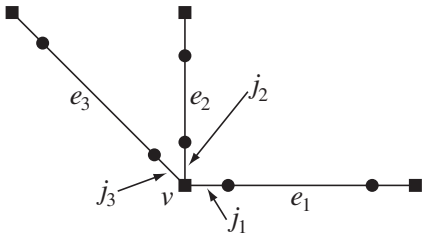

Figure 6: The members connected to node $v \in \tilde{\mathcal{V}}$.

We next consider the constraint imposing symmetry in configuration of the compliant mechanism. Suppose, for instance, the problem setting for generating a compliant converter; see Figure 2 in section 2.1. The horizontal external force is applied at the input node and the horizontal displacement of the output node is maximized. To guarantee that the output node has no vertical displacement, it might be natural to confine the feasible set to the set of structures that are symmetric with respect to the horizontal axis. Such a constraint can be formulated in terms of x_j's and y_j's as follows. Let $\mathcal{P}^{\mathrm{J}}_{\mathrm{sym}}$ denote the set of pairs of joint elements that are located at symmetric positions. That is, we write $(j, j') \in \mathcal{P}^{\mathrm{J}}_{\mathrm{sym}}$ if joint element $j \in \mathcal{E}^{\mathrm{J}}$ is swapped with joint element $j' \in \mathcal{E}^{\mathrm{J}}$ by the horizontal reflection. Then these two joint elements should have the same cross-section, which can be written as

$$(x_j, y_j) = (x_{j'}, y_{j'}), \quad \forall (j, j') \in \mathcal{P}^{\mathrm{J}}_{\mathrm{sym}}. \tag{39}$$

The next constraint aims to remove unnecessary members. Let $v \in \tilde{\mathcal{V}}$ be a ground node that is not either the input node or the output node. Suppose that only one member, denoted $\bar{e} \in \tilde{\mathcal{E}}$, is connected to node v. The specified external force is applied at the input node and no external force is applied at node v. From the balance of forces at node v it follows that member $\bar{e}$ has no internal stress at the equilibrium state. Therefore, the equilibrium configuration of the whole structure (and hence the objective value also) undergoes no change if member $\bar{e}$ is removed. In other words, such a member is unnecessary. This motivates us to consider the constraint such that node v has either (i) at least two members; or (ii) no members. This constraint can be formulated in terms of z_e's as follows. Let $\tilde{\mathcal{E}}(v) \subseteq \tilde{\mathcal{E}}$ denote the set of the ground members that are connected to node $v \in \tilde{\mathcal{V}}$. For instance, $\tilde{\mathcal{E}}(v) = \{e_1, e_2, e_3\}$ for the example shown in Figure 6. Then the number of existing members connecting to node v is given by

$$\sum_{e' \in \tilde{\mathcal{E}}(v)} z_{e'}.$$

From this observation, the constraint under consideration can be written as

$$2z_e \leq \sum_{e' \in \tilde{\mathcal{E}}(v)} z_{e'}, \quad \forall e \in \tilde{\mathcal{E}}(v) \tag{40}$$

for all $v \in \tilde{\mathcal{V}}$ except for the input and output nodes. Indeed, if no member remains, then $z_e = 0$ ($\forall e \in \tilde{\mathcal{E}}(v)$) and (40) is satisfied. On the other hand, suppose that there exist some remained members around node v. Let one of them denote $\hat{e} \in \tilde{\mathcal{E}}(v)$. Then $z_{\hat{e}} = 1$, and thence (40) reads $2z_{\hat{e}} = 2 \leq \sum_{e' \in \tilde{\mathcal{E}}(v)} z_{e'}$, which means that there remain at least two members around node v.

The final one is an optional constraint, that might be, however, somewhat meaningful from a viewpoint of manufacturability or robustness of compliant mechanisms. Namely, we can limit the number of elastic hinges around each node. More precisely, we can consider the upper bound constraint for the number of flexible joint elements, i.e., joint elements belonging $\mathcal{J}_{\text{flex}}$, that are connected to each node. Concentration of many flexible joint elements at one ground node may possibly cause difficulty of manufacture, yield instability around the node, and/or result in less immunity against failure. Suppose, for instance, that the upper bound under consideration is one. Let $\mathcal{E}^{\text{J}}(v) \subseteq \mathcal{E}^{\text{J}}$ denote the set of the joint elements that are connected to node $v \in \tilde{\mathcal{V}}$. For instance, in the case of Figure 6 we have that $\mathcal{E}^{\text{J}}(v) = \{j_1, j_2, j_3\}$. Then the constraint under consideration can be written as

$$\sum_{j \in \mathcal{E}^{\text{J}}(v)} y_j \leq 1, \quad \forall v \in \tilde{\mathcal{V}}, \tag{41}$$

because $y_j = 1$ means $j \in \mathcal{J}_{\text{flex}}$.

All these additional constraints, i.e., (38), (39), (40), and (41), are linear constraints. Hence, problem (37) with these additional constraints can still be handled within the framework of MILP. Thus various combinatorial constraints are dealt with easily, which might be one of advantages of the MILP approach.

Remark 3.1. In the presented method, the upper bound constraint for the structural volume can also be dealt with. To see this, we first consider the volume of a ground member. Recall that ground member $e \in \tilde{\mathcal{E}}$ has cross-sectional area $\bar{a}^{\text{s}}$ and its existence is expressed by $z_e \in \{0, 1\}$. Therefore, the volume of ground member e is given by

$$z_e \bar{a}^{\text{s}} \tilde{l}_e,$$

where $\tilde{l}_e$ is the member length. We next consider a joint element. By using (2) and (20), we see that the cross-sectional area of joint element $j \in \mathcal{E}^{\text{J}}$ can be represented as $x_j \bar{a}^{\text{s}} + y_j \bar{a}^{\text{f}}$. Hence, the volume is written as

$$(x_j \bar{a}^{\text{s}} + y_j \bar{a}^{\text{f}}) l_j.$$

By summing up these observations, we see that the volume constraint can be formulated as

$$\sum_{e \in \tilde{\mathcal{E}}} z_e \bar{a}^{\text{s}} \tilde{l}_e + \sum_{e \in \mathcal{E}^{\text{J}}} (x_j \bar{a}^{\text{s}} + y_j \bar{a}^{\text{f}}) l_j \leq \bar{V}, \tag{42}$$

where $\bar{V}$ is the specified upper bound for the structural volume. Thus the volume constraint can be represented as a linear inequality constraint. In our numerical experiments, however, constraint (42) is not added to problem (37). This is because, contrary to the compliance optimization, increase of $\bar{V}$ does not necessarily imply improvement of performance of a compliant mechanism. ■

4 Local search

In section 3, we have proposed to solve an MILP problem, (37), by using an existing algorithm with guaranteed global optimality. In practice, however, this approach might be applicable only when the number of design variables is relatively small.

This section presents a local search that can be applied to large-scale problems. This method solves a sequence of MILP subproblems, each of which finds the best one among feasible solutions in a specified neighborhood of the incumbent solution. Such sequential MILP methods were applied to topology optimization of continua [49] and frame structures [25]. An initial solution for this optimization process may be obtained by solving a problem for a coarse ground structure with a global optimization approach. Then we translate the obtained optimal solution onto a finer ground structure to obtain an initial solution for the local search. This procedure may be repeated until the current ground structure becomes sufficiently fine. Such hierarchical optimization methods for topology optimization were initiated in [49, 51]. Unlike the methods cited above, the local search proposed in the following uses two different types of neighborhoods alternately. That is, one is fixing structural topology and allowing only variation of sizes of structural elements, while the other allowing change in topology but restricting the amount of variation in solutions.

Recall that, in our formulation, the structural design is essentially determined only by $(x_j, y_j) \in \{0,1\}^2$ $(\forall j \in \mathcal{E}^{\mathrm{J}})$; see, e.g., (20) in section 3.2. Therefore, in the following we use $(\boldsymbol{x}, \boldsymbol{y})$ to represent a solution.

Let $(\boldsymbol{x}^*, \boldsymbol{y}^*)$ denote a current solution. For instance, at the first iteration of the sequential search, $(\boldsymbol{x}^*, \boldsymbol{y}^*)$ is the initial solution translated from the optimal solution for the coarser extended ground structure. We define two types of neighborhoods of $(\boldsymbol{x}^*, \boldsymbol{y}^*)$. First, define set $\hat{\mathcal{N}}(\boldsymbol{x}^*, \boldsymbol{y}^*) \subseteq \mathbb{R}^{2|\mathcal{E}^{\mathrm{J}}|}$ by

$$\hat{\mathcal{N}}(\boldsymbol{x}^*, \boldsymbol{y}^*) = \{(\boldsymbol{x}, \boldsymbol{y}) \mid \boldsymbol{x} + \boldsymbol{y} = \boldsymbol{x}^* + \boldsymbol{y}^*,\ (x_j, y_j) \in \{0,1\}^2\ (\forall j \in \mathcal{E}^{\mathrm{J}})\}.$$

Second, for a given radius $r > 0$, define set $\check{\mathcal{N}}(\boldsymbol{x}^*, \boldsymbol{y}^*; r) \subseteq \mathbb{R}^{2|\mathcal{E}^{\mathrm{J}}|}$ by

$$\check{\mathcal{N}}(\boldsymbol{x}^*, \boldsymbol{y}^*; r) = \{(\boldsymbol{x}, \boldsymbol{y}) \mid \|\boldsymbol{x} - \boldsymbol{x}^*\|_1 + \|\boldsymbol{y} - \boldsymbol{y}^*\|_1 \leq r,\ (x_j, y_j) \in \{0,1\}^2\ (\forall j \in \mathcal{E}^{\mathrm{J}})\}.$$

It is worth noting that $\hat{\mathcal{N}}(\boldsymbol{x}^*, \boldsymbol{y}^*)$ is the set of solutions that have the same topology as $(\boldsymbol{x}^*, \boldsymbol{y}^*)$. Within this neighborhood, joint element $j \in \mathcal{J}_{\mathrm{stiff}}$ at the current solution is allowed to change as $j \in \mathcal{J}_{\mathrm{flex}}$, and joint element $j' \in \mathcal{J}_{\mathrm{flex}}$ is allowed to change as $j' \in \mathcal{J}_{\mathrm{stiff}}$. In contrast, $\check{\mathcal{N}}(\boldsymbol{x}^*, \boldsymbol{y}^*; r)$ allows addition and removal of joint elements. Instead, the number of different components between $(\boldsymbol{x}, \boldsymbol{y})$ and $(\boldsymbol{x}^*, \boldsymbol{y}^*)$ is restricted up to r. We propose a local search that uses these two different neighborhoods alternately.

The sequential MILP method based upon the local search using these two neighborhoods is described as follows.

Algorithm 4.1.

Step 0 Translate the solution for the coarser extended ground structure to the current extended ground structure. Let $(\check{\boldsymbol{x}}^{(0)}, \check{\boldsymbol{y}}^{(0)})$ and $\hat{f}^{(0)}$ denote the translated solution and the objective value, respectively. Choose positive integer r. Set $k = 0$.

Step 1 Solve the MILP problem with the constraint $(\boldsymbol{x}, \boldsymbol{y}) \in \hat{\mathcal{N}}(\check{\boldsymbol{x}}^{(k)}, \check{\boldsymbol{y}}^{(k)})$. Let $(\hat{\boldsymbol{x}}^{(k+1)}, \hat{\boldsymbol{y}}^{(k+1)})$ and $\hat{f}^{(k+1)}$ denote the optimal solution and the optimal value, respectively.

Step 2 If $\hat{f}^{(k)} < \hat{f}^{(k+1)}$, then go to step 4. Otherwise, go to step 3.

Step 3 Check the stresses of the existing members. If all the members have nonzero stresses, then declare $(\hat{\boldsymbol{x}}^{(k+1)}, \hat{\boldsymbol{y}}^{(k+1)})$ as the solution and terminate. Otherwise, remove the members

that have no stresses, let anew $(\hat{\boldsymbol{x}}^{(k+1)}, \hat{\boldsymbol{y}}^{(k+1)})$ denote the obtained solution, and go to step 4.

Step 4 Solve the MILP problem with the constraint $(\boldsymbol{x}, \boldsymbol{y}) \in \check{\mathcal{N}}(\hat{\boldsymbol{x}}^{(k+1)}, \hat{\boldsymbol{y}}^{(k+1)}; r)$. Let $(\check{\boldsymbol{x}}^{(k+1)}, \check{\boldsymbol{y}}^{(k+1)})$ denote the optimal solution. Update $k \leftarrow k+1$ and go to step 1.

■

Remark 4.2. At step 1 of Algorithm 4.1, the feasible set is restricted within $\hat{\mathcal{N}}(\check{\boldsymbol{x}}^{(k)}, \check{\boldsymbol{y}}^{(k)})$. In view of (37i), define $\check{z}_e$ $(\forall e \in \tilde{\mathcal{E}})$ by

$$\check{z}_e = \check{x}^{(k)}_{j_1(e)} + \check{y}^{(k)}_{j_1(e)}.$$

Then this restriction is equivalent to adding the constraints

$$z_e = \check{z}_e, \quad \forall e \in \tilde{\mathcal{E}}.$$

That is, variables z_e's are fixed. Define $\mathrm{supp}(\check{\boldsymbol{z}}) \subseteq \tilde{\mathcal{E}}$ by

$$\mathrm{supp}(\check{\boldsymbol{z}}) = \{e \in \tilde{\mathcal{E}} \mid \check{z}_e = 1\}.$$

Then constraint (37h) can be replaced by

$$|\tilde{c}_e - \tilde{\boldsymbol{b}}^{\top}_{e,t} \boldsymbol{u}| \leq 0, \quad \forall e \in \mathrm{supp}(\check{\boldsymbol{z}}).$$

As a consequence, at step 1 we solve an MILP problem which does not include big constant M. It is known that presence of such a large constant, called "big-M," in an MILP problem often slows down the solution process, because it weakens relaxation problems of the MILP problem. The subproblem at step 1 does not have this weak point. Therefore, it is expected that this problem can be solved with quite small computational cost, although, unlike the subproblem at step 4, no limitation is imposed on the amount of variation from the incumbent solution. Indeed, this expectation is supported by the numerical results in section 5.2.2. The subproblem solved at step 4 uses neighborhood $\check{\mathcal{N}}(\boldsymbol{x}^*, \boldsymbol{y}^*; r)$ and involves big-M. There exists trade-off relation that the local search using only this subproblem might possibly converge to a poor local optimal when r is small, while computational cost often increases drastically as r increases. In view of these issues this paper uses two neighborhoods alternately, rather than increasing r at step 4, to achieve diversity of the solutions explored within one iteration of the local search and to retain relatively small computational cost. ■

Remark 4.3. At step 2 of Algorithm 4.1, if $\hat{f}^{(k+1)}$ does not satisfy $\hat{f}^{(k)} < \hat{f}^{(k+1)}$, then $\hat{f}^{(k)} = \hat{f}^{(k+1)}$ holds. ■

Remark 4.4. At step 3 of Algorithm 4.1, we remove, if any, the members that have zero stresses at the equilibrium state subjected to the input force. This procedure may possibly enlarge the solution space explored by the algorithm, because the solution obtained at step 3 does no longer belong to $\hat{\mathcal{N}}(\check{\boldsymbol{x}}^{(k)}, \check{\boldsymbol{y}}^{(k)})$. In our numerical experiments, such a case actually appears; see example (V) in section 5.2.2. ■

Remark 4.5. At step 4 of Algorithm 4.1, the feasible set is restricted within $\check{\mathcal{N}}(\hat{\boldsymbol{x}}^{(k+1)}, \hat{\boldsymbol{y}}^{(k+1)}; r)$. This constraint can be expressed by a linear inequality. Indeed, the constraint is equivalently rewritten as

$$\sum_{j \in \mathrm{supp}(\hat{\boldsymbol{x}}^{(k+1)})} (1 - x_j) + \sum_{j \notin \mathrm{supp}(\hat{\boldsymbol{x}}^{(k+1)})} x_j + \sum_{j \in \mathrm{supp}(\hat{\boldsymbol{y}}^{(k+1)})} (1 - y_j) + \sum_{j \notin \mathrm{supp}(\hat{\boldsymbol{y}}^{(k+1)})} y_j \leq r.$$

Therefore, the problem solved at step 4 is an MILP problem. ■

5 Numerical experiments

Compliant mechanisms with standardized sections were generated by solving problem (37) with the additional constraints, (38), (39), (40), and (41). Computation was carried out on two 2.66 GHz 6-Core Intel Xeon Westmere processors with 64 GB RAM. MILP problems were solved by using CPLEX ver. 12.2 [21], where the data of the problems were prepared in the CPLEX LP file format. The integrality tolerance in CPLEX is set to 0 and the feasibility tolerance in the simplex method is set to 10^{-8}. The other parameters of CPLEX are set to the default values.

As for material parameters, Young's modulus and Poisson's ratio are $E = 70\,\mathrm{GPa}$ and $\nu = 0.4$, respectively. The shear modulus is thence $G = E/2(1+\nu) = 25\,\mathrm{MPa}$. The upper bound for stress in constraints (37c) and (37d) is $\bar{\sigma} = 3.4\,\mathrm{GPa}$.

Each ground member has a rectangular cross-section with width $w = 5\,\mathrm{mm}$ and thickness $t = 1\,\mathrm{mm}$. The joint elements belonging to $\mathcal{J}_{\mathrm{stiff}}$ have the same section as a ground member. For the flexible joint elements, i.e., the ones belonging to $\mathcal{J}_{\mathrm{flex}}$, the moment of inertia and the elastic section modulus are 1/25 and 1/5 of the values of the ground members. respectively. The shear correction factor in the Timishenko beam theory is $\kappa = 5/6$. The input force applied at the input node is $f_{\mathrm{in}} = 100\,\mathrm{N}$. The elongation stiffness of the output spring is $28\,\mathrm{kN/m}$.

5.1 Global optimization with single mixed-integer programming

This section collects relatively small examples. For these examples, the global optimal solution of the proposed MILP problem can be found with small computational effort.

5.1.1 Example (I)

Consider an inverter problem shown in Figure 2 in section 2.2, where $L = 25\,\mathrm{mm}$. The extended ground structure consists of $\tilde{\mathcal{E}} = 28$ ground members and $|\mathcal{E}^{\mathrm{J}}| = 56$ joint elements. The ground nodes are depicted as filled squares in Figure 2. The length of each joint element is $L/16$. The configuration of a compliant mechanism is assumed to have symmetry with respect to reflection across the horizontal center line.

Computational results are listed in Table 2. Here, u_{out} is the optimal value, u_{in} is the displacement of the input node caused by the input force, and "time" reports the computational time spent by CPLEX [21]. The optimal solution and its deformed configuration are shown in Figure 7. This solution has four flexible joint elements. Note that the rightmost node and the leftmost node in the middle row have no flexible joint elements. As mentioned in section 3.4, we consider the upper bound constraint for the number of flexible joint elements around a ground node; i.e., each

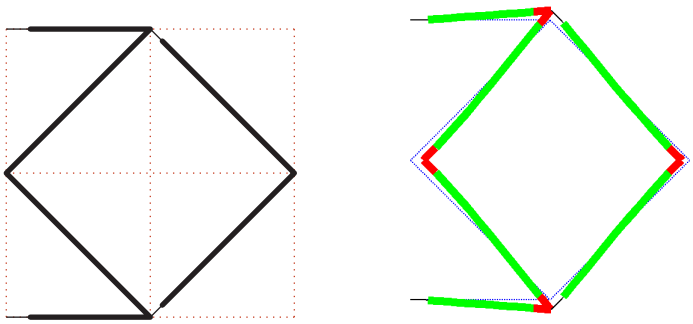

(a) (b)

Figure 7: Example (I). (a) The optimal solution; and (b) its deformed configuration (displacements are magnified 50 times).

ground node can have at most one flexible joint element.[2] Due to this constraint and the symmetry constraint, these two nodes cannot have a flexible joint. The objective value could be improved if the four joint elements connected to these two nodes are replaced by flexible ones. In view of this aspect the result in Figure 7 agrees with the results in literature [22, 30, 59].

5.1.2 Example (II)

We next consider a problem setting shown in Figure 8(a). The members depicted by solid lines are supposed to have the joint elements belonging to $\mathcal{J}_{\text{stiff}}$; their shapes are fixed. The members depicted by dotted lines are considered targets of design. Accordingly, the number of the joint elements to be designed is 78. An output spring is connected to the two output nodes. The configuration of a compliant mechanism is assumed to have symmetry with respect to reflection across the horizontal center line. The length parameter of the design domain is $L = 75\,\text{mm}$. The length of each joint element is $L/32$.

Figure 8(b) shows the optimal solution. This structure has 10 flexible joint elements. The deformed configuration is shown in Figure 8(c). Computational results are listed in Table 2.

5.1.3 Example (III)

Figure 9(a) shows the ground structure and boundary conditions to design a compliant gripper. We use the same ground structure as example (II). Only difference is the direction of the input force. The dotted lines show the members that are to be designed. No flexible joints are made in the

Table 2: Computational results of examples (I), (II), and (III).

	u_{out} (mm)	$u_{\text{out}}/u_{\text{in}}$	Time (s)
Example (I)	0.09367	0.46572	8.3
Example (II)	0.45673	1.47508	20.0
Example (III)	0.10112	0.29035	229.3

[2]This is an optional constraint as explained section 3.4.

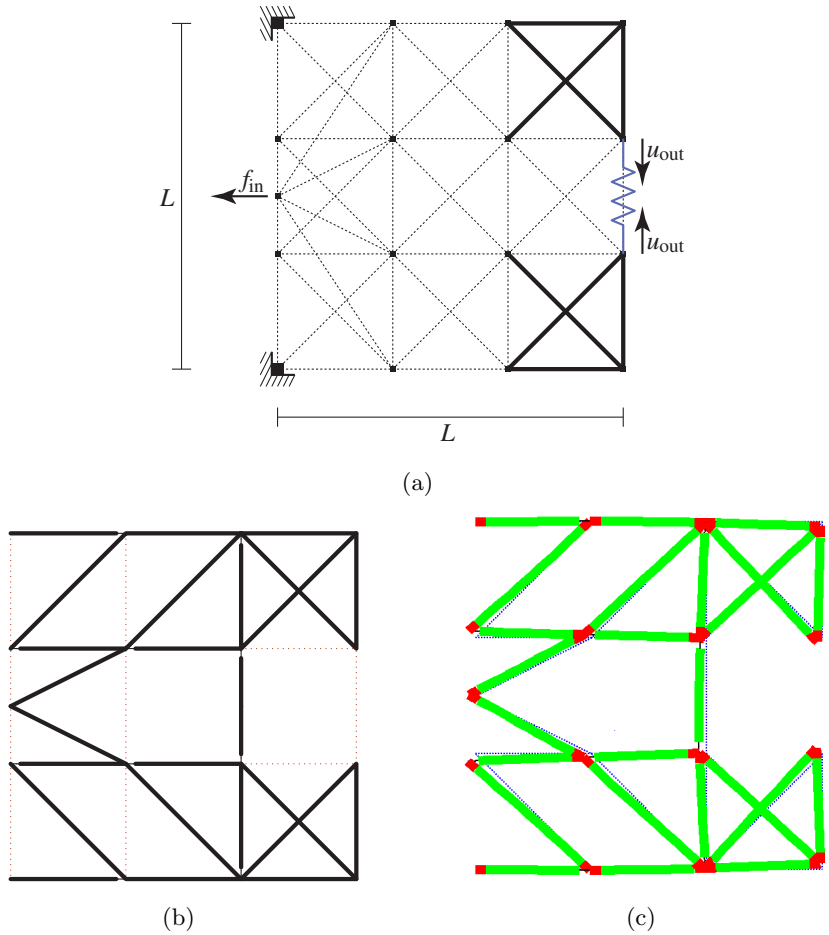

Figure 8: Example (II). (a) The design domain and boundary condition; (b) the optimal solution; and (c) the deformed configuration of the optimal solution (displacements are magnified 50 times).

members depicted by the solid lines; the shapes of these members are fixed. We also consider the symmetry constraint with respect to the reflection across the horizontal centerline.

Figure 9(b) shows the optimal solution, which has 8 flexible joint elements. Figure 9(c) depicts the deformed configuration. As observed from Table 2, the output displacement is not very large, compared with the input displacement. This motivates us to try to solve the same problem with a finer ground structure. To do this, in section 5.2 we adopt the local search presented in section 4.

5.2 Larger examples with sequential mixed-integer programming

In this section problems with many design variables are solved by using Algorithm 4.1 in section 4.

5.2.1 Example (IV)

Figure 10(a) shows a ground structure consisting of $|\mathcal{V}| = 49$ nodes and 276 members. The cross-sections of members depicted by solid lines (i.e., 16 joint elements) are designated to belong to $\mathcal{J}_{\text{stiff}}$. The number of joint members to be designed is 520 and the number of the corresponding ground members is 260. The length of each side of the design domain is $L = 75\,\text{mm}$ and the length of each

[3]The solution obtained at the 6th iteration is same as those at the 5th iteration.

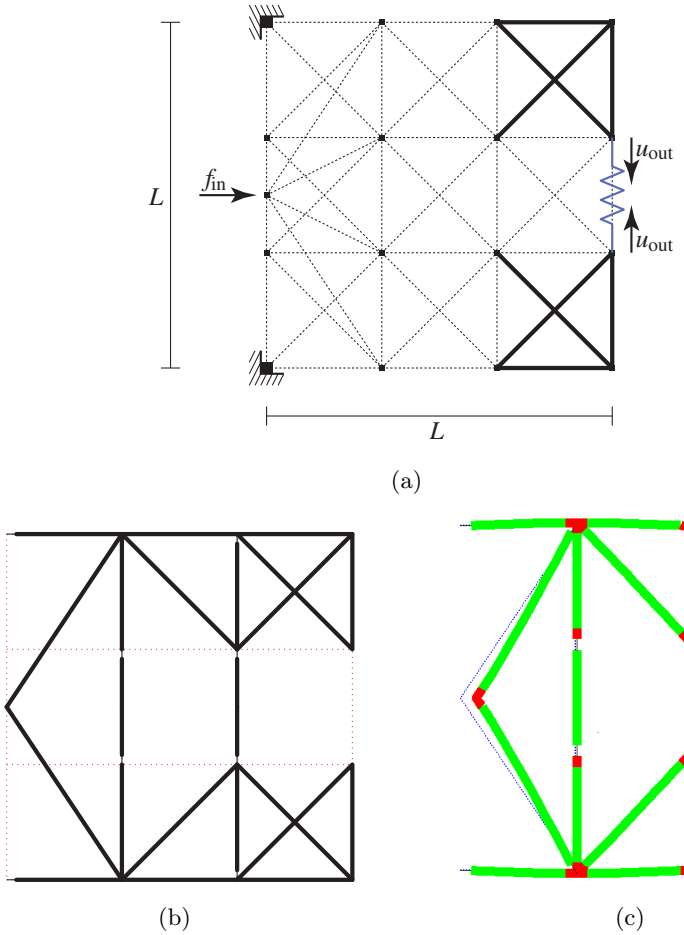

Figure 9: Example (III). (a) The design domain and boundary condition; (b) the optimal solution; and (c) the deformed configuration of the optimal solution (displacements are magnified 50 times).

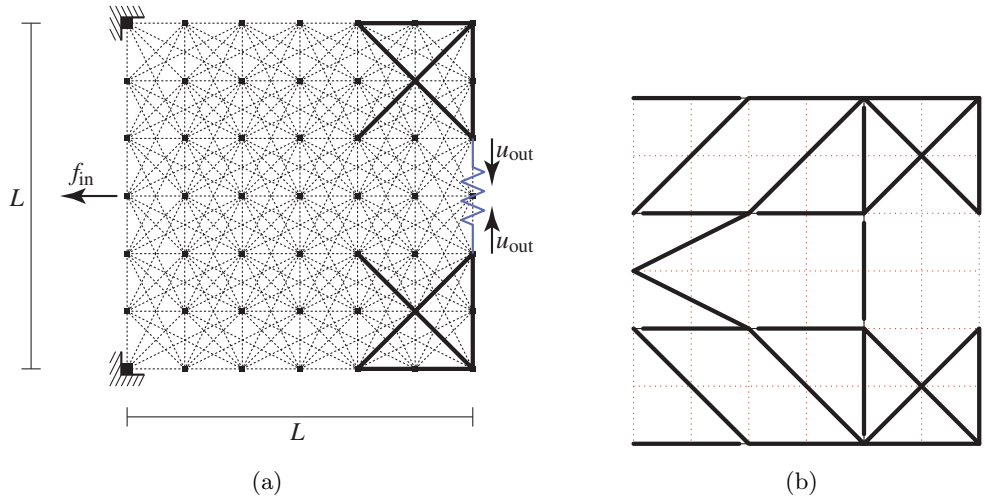

Figure 10: Example (IV). (a) The design domain and boundary condition; and (b) the initial solution.

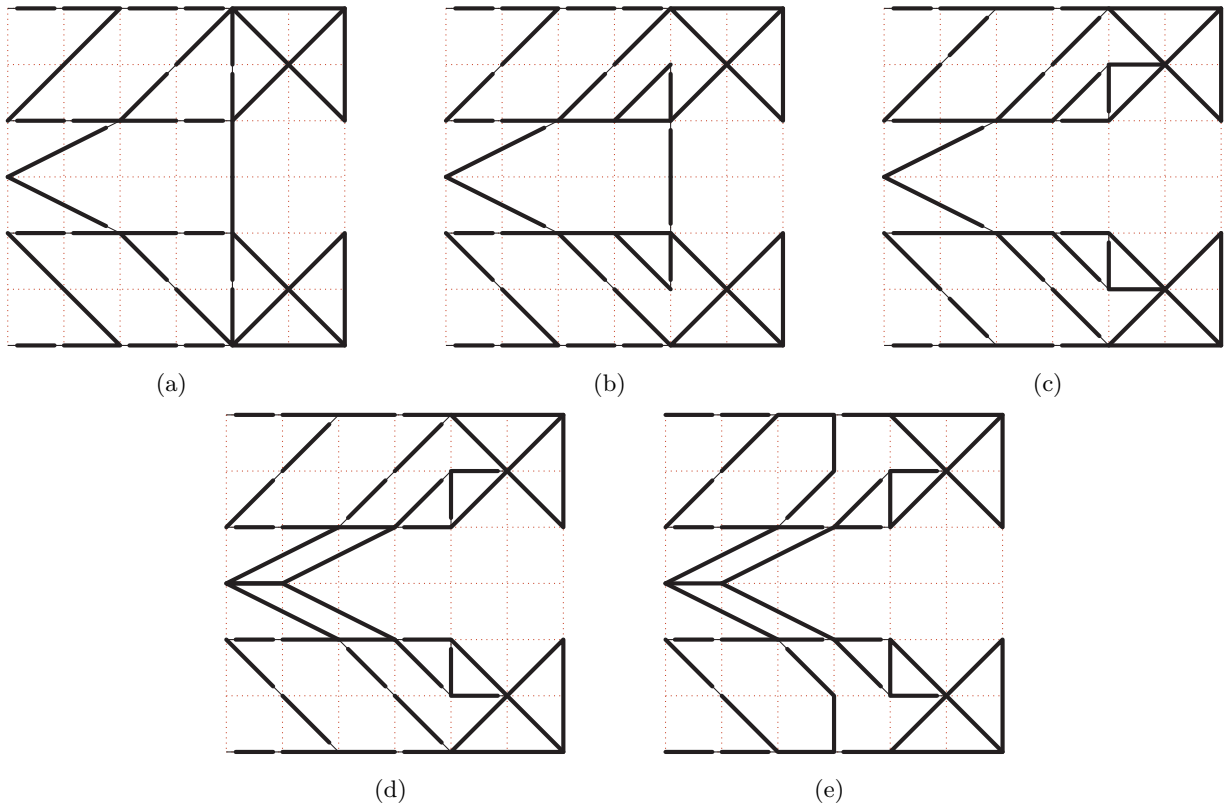

Figure 11: Convergence history of example (IV). The solutions obtained at (a) the 1st iteration; (b) the 2nd iteration; (c) the 3rd iteration; (d) the 4th iteration; and (e) the 5th iteration.

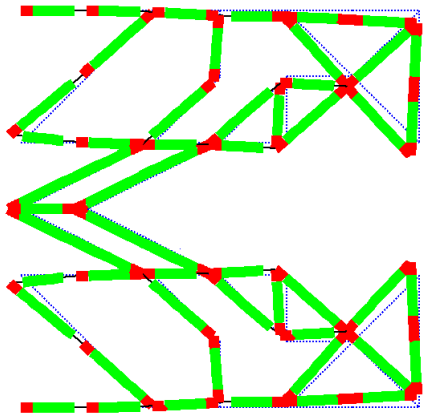

Figure 12: The deformed configuration of the obtained solution of example (IV) (displacements are magnified 50 times).

joint element is $L/32$.

For this problem, example (II) in section 5.1.2 serves as a preceding coarse case in the hierarchical optimization algorithm. The optimal solution of example (II) can be translated to the current ground structure as shown in Figure 10(b). This solution is adopted as the initial point for Algorithm 4.1. The radius of the neighborhood used at step 3 of Algorithm 4.1 is $r = 8$.

Algorithm 4.1 terminates after 6 iterations, i.e., a convergent solution is obtained after 5 iterations. The convergence history is shown in Figure 11, where $(\hat{\boldsymbol{x}}^{(k)}, \hat{\boldsymbol{y}}^{(k)})$, i.e., the solution obtained at step 1 of Algorithm 4.1, at each iteration is illustrated. The deformation of the obtained solution is shown in Figure 12. Computational results are listed in Table 3. Since we solve two MILP problems at each iteration, both results are reported in Table 3. The objective value of the obtained solution is about 2.1 times larger than that of the initial solution.

5.2.2 Example (V)

The final example is shown in Figure 13(a). This ground structure is same as example (IV). Only the direction of the input force is reversed. For this problem, example (III) in section 5.1.3 serves as a preceding coarse case in the hierarchical optimization algorithm. Figure 13(b) shows the initial solution for Algorithm 4.1, i.e., the solution translated from example (III) to the current problem setting. The radius of the neighborhood used at step 3 of Algorithm 4.1 is $r = 8$.

Algorithm 4.1 terminates after 10 iterations. Figure 14 shows the convergence history. At step 3 of the 6th iteration, 7 members in Figure 14(e) are found to have no stresses at the equilibrium state. These members are removed, which results in the solution shown in Figure 14(f). At the other iterations, all members have nonzero stresses and, hence, the solution at step 3 is same as that at step 1. Figure 15 depicts the deformation of the obtained solution. It can be observed that the deformation is primarily induced by bending at flexible joint elements. Computational results are

Table 3: Computational results of example (IV).[3]

Iter.	u_{out} (mm)	$u_{\text{out}}/u_{\text{in}}$	Time (s)
0	0.45673	1.47508	—
1: step 1	0.51252	1.61826	436.4
1: step 4	0.60924	1.49989	563.8
2: step 1	0.65351	1.57438	440.8
2: step 4	0.88402	2.09697	543.6
3: step 1	0.88902	2.07038	909.1
3: step 4	0.91154	2.17313	918.4
4: step 1	0.91929	2.16676	7,245.0
4: step 4	0.93081	2.00230	481.0
5: step 1	0.94956	2.01114	2,464.9
5: step 4	0.94956	2.01114	540.7
6: step 1	0.94956	2.01114	2,465.7

[4]The solution obtained at the 10th iteration is same as the ones at the 9th iteration.

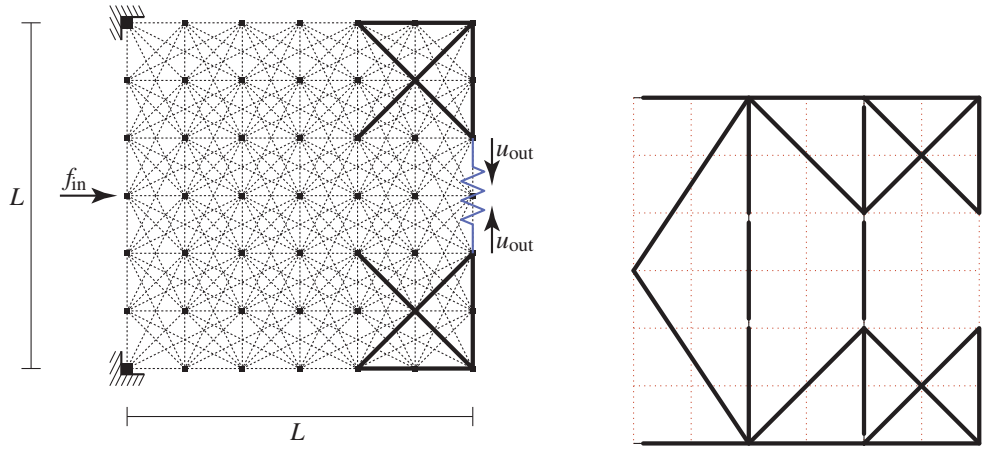

(a) (b)

Figure 13: Example (V). (a) The design domain and boundary condition; and (b) the initial solution.

Table 4: Computational results of example (V).[4]

Iter.	u_{out} (mm)	$u_{\text{out}}/u_{\text{in}}$	Time (s)
0	0.10112	0.29035	—
1: step 1	0.10490	0.30484	36.5
1: step 4	0.10893	0.37150	1,343.5
2: step 1	0.10893	0.37150	65.7
2: step 4	0.13037	0.28754	1,135.5
3: step 1	0.13884	0.28325	70.0
3: step 4	0.14009	0.29251	1,582.7
4: step 1	0.14100	0.29320	208.2
4: step 4	0.21345	0.64703	1,765.1
5: step 1	0.21762	0.64677	67.6
5: step 4	0.21762	0.64677	1,329.2
6: step 1	0.21762	0.64677	67.6
6: step 4	0.27879	0.60534	1,145.0
7: step 1	0.34337	0.63488	30.5
7: step 4	0.48386	1.22008	415.4
8: step 1	0.55127	1.23219	23.9
8: step 4	0.60738	1.55575	714.7
9: step 1	0.72660	1.64941	31.5
9: step 4	0.72660	1.64941	608.1
10: step 1	0.72660	1.64941	31.5

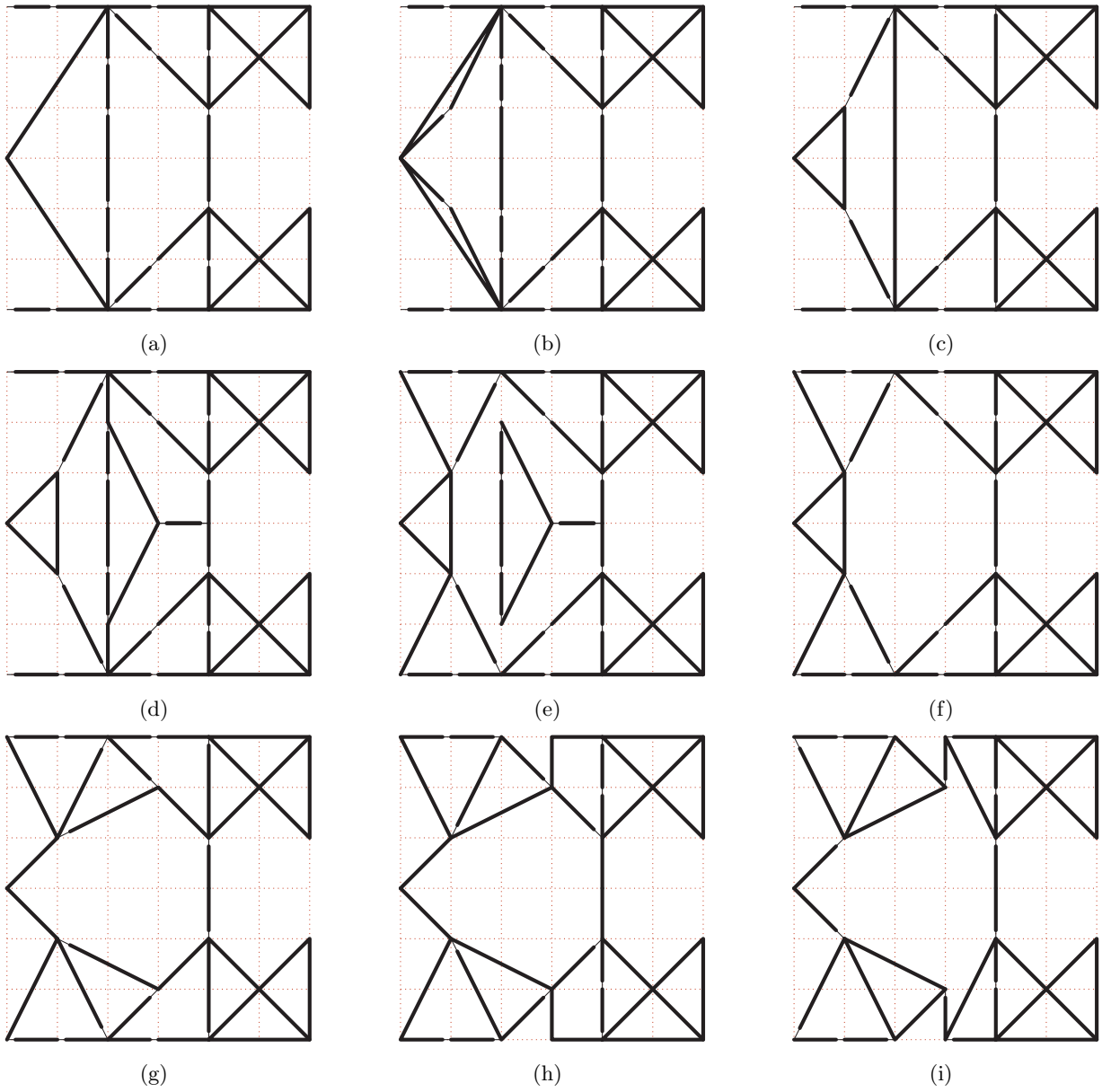

Figure 14: Convergence history of example (V). The solutions obtained at (a) the 1st iteration; (b) the 2nd iteration; (c) the 3rd iteration; (d) the 4th iteration; (e) step 1 of the 5th iteration; (f) step 3 of the 5th iteration; (g) the 7th iteration; (h) the 8th iteration; and (i) the 9th iteration.

listed in Table 4. The objective value of the obtained solution is about 7.2 times larger than that of the initial solution. Also, topology of the final solution (in Figure 14(i)) is much different from that of the initial solution (in Figure 13(b)). Thus the local search can improve the initial solution substantially. The effect of using the two different neighborhoods in the local search may be observed from Figure 14 and Table 4. From the viewpoint of the solution space explored at one iteration, it may be seen that variations, among others, from Figures 14(b) to 14(c), from Figures 14(f) to 14(g), and from Figures 14(g) to 14(h) are much larger than the range of $\check{\mathcal{N}}(\boldsymbol{x}^*, \boldsymbol{y}^*; r)$ with $r = 8$. Thus making use of both $\check{\mathcal{N}}(\boldsymbol{x}^*, \boldsymbol{y}^*; r)$ and $\hat{\mathcal{N}}(\check{\boldsymbol{x}}^*, \check{\boldsymbol{y}}^*)$ enlarges the solution space explored at one iteration of the local search. Meanwhile, it is observed from Table 4 that the computational effort for solving a subproblem defined with $\hat{\mathcal{N}}(\check{\boldsymbol{x}}^*, \check{\boldsymbol{y}}^*)$ is much smaller than that for solving a subproblem with

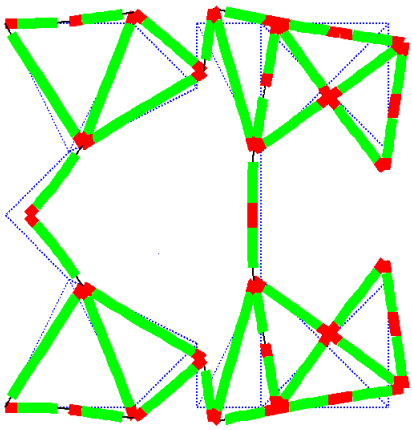

Figure 15: The deformed configuration of the obtained solution of example (V) (displacements are magnified 50 times).

$\check{\mathcal{N}}(\boldsymbol{x}^*, \boldsymbol{y}^*; 8)$. This is because, as discussed in Remark 4.2, the subproblem defined with $\hat{\mathcal{N}}(\check{\boldsymbol{x}}^*, \check{\boldsymbol{y}}^*)$ does not involve "big-M." Thus using the two neighborhoods has an advantage in computational efficiency compared with using only $\check{\mathcal{N}}(\boldsymbol{x}^*, \boldsymbol{y}^*; r)$ with an increased value of r.

6 Conclusions

Generous studies are being made to optimization methods, mostly continuum-based topology optimization methods, for design of compliant mechanisms. This paper has explored potentials of a mixed-integer programming approach to designing compliant mechanisms that are realized as planar frame structures consisting of standardized beam elements. To give some joints rotational flexibility and allow variation of structural topology, we have adopted element-connectivity parameterization due to Jang *et al.* [22], in which the cross-sections of two short joint elements connected to both ends of each ground beam are considered design variables. In this paper, sections not only of the ground members but also of the joints elements are standardized, i.e., the design variables are chosen among predetermined candidates. The local stress constraints are directly addressed. By maximizing the output displacement under these constraints, we have attempted to balancing the two objectives, preventing local failures and gaining flexibility that induces the desired performance as a compliant mechanism. As a consequence, the obtained solution has no hinge-like regions and the cross-sections of its elements are fully standardized. This might make it easy to manufacture physical products without resorting to post-processing of the computational results. Also, the locations of elastic hinges are clearly identified in the solution and, hence, from a mechanical point of view one might easily grasp essential points of the obtained design.

The proposed method solves a mixed-integer linear programming (MILP) problem to find a compliant mechanism. Small-scale problems can be solved by using an existing algorithm with guaranteed convergence to global optimal solutions. Larger problems have been attacked by a local search, in which MILP problems, in conjunction with the constraint restricting the solution space, are solved sequentially. This local search uses two different kinds of neighborhoods alternately in order to permit sufficient variation of structural topology and achieve relatively small computational

cost. The solution obtained by the local search is not guaranteed to be globally optimal but satisfies the local stress constraints.

This paper has developed an MILP formulation for topology optimization of frame structures with an element-connectivity parameterization. For continuum optimization with this parameterization [58, 60], a similar MILP formulation is possible. Also, extension to optimization of a frame model with flexible joints [14, 15] could be explored.

Acknowledgments

The work of the second author is partially supported by Grant-in-Aid for Scientific Research (C) 26420545.

References

[1] Achterberg, T.: SCIP: Solving constraint integer programs. *Mathematical Programming Computation*, **1**, 1–41 (2009).

[2] Achtziger, W., Kanzow, C.: Mathematical programs with vanishing constraints: Optimality conditions and constraint qualifications. *Mathematical Programming*, **A114**, 69–99 (2008).

[3] Allaire, G., Jouve, F.: Minimum stress optimal design with the level set method. *Engineering Analysis with Boundary Elements*, **32**, 909–918 (2008).

[4] Bruggi, M.: On an alternative approach to stress constraints relaxation in topology optimization. *Structural and Multidisciplinary Optimization*, **36**, 125–141 (2008).

[5] Bruns, T.E., Tortorelli, D.A.: Topology optimization of non-linear elastic structures and compliant mechanisms. *Computer Methods in Applied Mechanics and Engineering*, **190**, 3443–3459 (2001).

[6] Cheng, G.: Some aspects of truss topology optimization. *Structural Optimization*, **10**, 173–179 (1995).

[7] Cheng, G.D., Guo, X.: ε-relaxed approach in structural topology optimization. *Structural Optimization*, **13**, 258–266 (1997).

[8] Danna, E., Rothberg, E., Le Pape, C.: Exploring relaxation induced neighborhoods to improve MIP solutions. *Mathematical Programming*, **102**, 71–90 (2005).

[9] De Franceschi, R., Fischetti, M., Toth, P.: A new ILP-based refinement heuristic for vehicle routing problems. *Mathematical Programming*, **105**, 471–499 (2006).

[10] Duysinx, P., Bendsøe, M.P.: Topology optimization of continuum structures with local stress constraints. *International Journal for Numerical Methods in Engineering*, **43**, 1453–1478 (1998).

[11] Erera, A., Hewitt, M., Savelsbergh, M., Zhang, Y.: Improved load plan design through integer programming based local search. *Transportation Science*, **47**, 412–427 (2013).

[12] Fischetti, M., Lodi, A.: Local branching. *Mathematical Programming*, **98**, 23–47 (2003).

[13] Frecker, M., Ananthasuresh, G.K., Nishiwaki, S., Kikuchi, N., Kota, S.: Topological synthesis of compliant mechanisms using multi-criteria optimization. *Journal of Mechanical Design (ASME)*, **119**, 238–245 (1997).

[14] Fredricson, H.: Topology optimization of frame structures—Joint penalty and material selection. *Structural and Multidisciplinary Optimization*, **30**, 193–200 (2005).

[15] Fredricson, H., Johansen, T., Klarbring, A., Petersson, J.: Topology optimization of frame structures with flexible joints. *Structural and Multidisciplinary Optimization*, **25**, 199–214 (2003).

[16] Gulczynski, D., Golden, B., Wasil, E.: The multi-depot split delivery vehicle routing problem: An integer programming-based heuristic, new test problems, and computational results. *Computers and Industrial Engineering*, **61**, 794–804 (2011).

[17] Guo, X., Zhang, W.S., Wang, M.Y., Wei, P.: Stress-related topology optimization via level set approach. *Computer Methods in Applied Mechanics and Engineering*, **200**, 3439–3452 (2011).

[18] Guo, X., Zhang, W., Zhong, W.: Stress-related topology optimization of continuum structures involving multi-phase materials. *Computer Methods in Applied Mechanics and Engineering*, **268**, 632–655 (2014).

[19] Hansen, P., Mladenović, N., Urošević, D.: Variable neighborhood search and local branching. *Computers and Operations Research*, **33**, 3034–3045 (2006).

[20] Holmberg, E., Torstenfelt, B., Klarbring, A.: Stress constrained topology optimization. *Structural and Multidisciplinary Optimization*, **48**, 33–47 (2013).

[21] IBM ILOG: *User's Manual for CPLEX*. `http://www.ilog.com/` (Accessed March 2014).

[22] Jang, G.-W., Kim, M.-J., Kim, Y.Y.: Design optimization of compliant mechanisms consisting of standardized elements. *Journal of Mechanical Design (ASME)*, **131**, 121006 (2009).

[23] Kanno, Y.: Exploring new tensegrity structures via mixed integer programming. *Structural and Multidisciplinary Optimization*, **48**, 95–114 (2013).

[24] Kanno, Y., Guo, X.: A mixed integer programming for robust truss topology optimization with stress constraints. *International Journal for Numerical Methods in Engineering*, **83**, 1675–1699 (2010).

[25] Kureta, R., Kanno, Y.: A mixed integer programming approach to designing periodic frame structures with negative Poisson's ratio. *Optimization and Engineering*, to appear. DOI: 10.1007/s11081-013-9225-7.

[26] Langelaar, M., Yoon, G.H., Kim, Y.Y., van Keulen, F.: Topology optimization of planar shape memory alloy thermal actuators using element connectivity parameterization. *International Journal for Numerical Methods in Engineering*, **88**, 817–840 (2011).

[27] Li, Y., Saitou, K., Kikuchi, N.: Topology optimization of thermally actuated compliant mechanisms considering time-transient effect. *Finite Elements in Analysis and Design*, **40**, 1317–1331 (2004).

[28] Lu, K.-J., Kota, S.: Topology and dimensional synthesis of compliant mechanisms using discrete optimization. *Journal of Mechanical Design (ASME)*, **128**, 1080–1091 (2006).

[29] Luo, J., Luo, Z, Chen, S, Tong, L., Wang, M.Y.: A new level set method for systematic design of hinge-free compliant mechanisms. *Computer Methods in Applied Mechanics and Engineering*, **198**, 318–331 (2008).

[30] Luo, Z., Tong, L.: A level set method for shape and topology optimization of large-displacement compliant mechanisms. *International Journal for Numerical Methods in Engineering*, **76**, 862–892 (2008).

[31] MacNeal, R.H.: A simple quadrilateral shell element. *Computers and Structures*, **8**, 175–183 (1978).

[32] Mei, Y., Wang, X.: A level set method for structural topology optimization and its applications. *Advances in Engineering Software*, **35**, 415–441 (2004).

[33] Nishiwaki, S., Frecker, M.I., Min, S., Kikuchi, N.: Topology optimization of compliant mechanisms using the homogenization method. *International Journal for Numerical Methods in Engineering*, **42**, 535–559 (1998).

[34] Parsons, R., Canfield, S.L.: Developing genetic programming techniques for the design of compliant mechanisms. *Structural and Multidisciplinary Optimization*, **24**, 78–86 (2002).

[35] Pedersen, C.B.W., Buhl, T., Sigmund, O.: Topology synthesis of large-displacement compliant mechanisms. *International Journal for Numerical Methods in Engineering*, **50**, 2683–2705 (2001).

[36] Poulsen, T.A.: A new scheme for imposing a minimum length scale in topology optimization. *International Journal for Numerical Methods in Engineering*, **57**, 741–760 (2003).

[37] Rahmatalla, S., Swan, C.C.: Sparse monolithic compliant mechanisms using continuum structural topology optimization. *International Journal for Numerical Methods in Engineering*, **62**, 1579–1605 (2005).

[38] Ramrakhyani, D.S., Frecker, M.I., Lesieutre, G.A.: Hinged beam elements for the topology design of compliant mechanisms using the ground structure approach. *Structural and Multidisciplinary Optimization*, **37**, 557–567 (2009).

[39] Rasmussen, M.H., Stolpe, M.: Global optimization of discrete truss topology design problems using a parallel cut-and-branch method. *Computers and Structures*, **86**, 1527–1538 (2008).

[40] Reddy, J.N.: On locking-free shear deformable beam finite elements. *Computer Methods in Applied Mechanics and Engineering*, **149**, 113–132 (1997).

[41] Rozvany, G.I.N.: On design-dependent constraints and singular topologies. *Structural and Multidisciplinary Optimization*, **21**, 164–172 (2001).

[42] Sauter, M., Kress, G., Giger, M., Ermanni, P.: Complex-shaped beam element and graph-based optimization of compliant mechanisms. *Structural and Multidisciplinary Optimization*, **36**, 429–442 (2008).

[43] Saxena, A.: Topology design of large displacement compliant mechanisms with multiple materials and multiple output ports. *Structural and Multidisciplinary Optimization.* **30** , 477–490 (2005).

[44] Saxena, A., Ananthasuresh, G.K.: Topology optimization of compliant mechanisms with strength considerations. *Mechanics of Structures and Machines*, **29**, 199–221 (2001).

[45] Sigmund, O.: On the design of compliant mechanisms using topology optimization. *Mechanics of Structures and Machines*, **25**, 493–524 (1997).

[46] Sigmund, O.: Design of multiphysics actuators using topology optimization—Part I: One-material structures. *Computer Methods in Applied Mechanics and Engineering*, **190**, 6577–6604 (2001).

[47] Sigmund, O.: Morphology-based black and white filters for topology optimization. *Structural and Multidisciplinary Optimization*, **33**, 401–424 (2007).

[48] Stolpe, M.: On the reformulation of topology optimization problems as linear or convex quadratic mixed 0–1 programs. *Optimization and Engineering*, **8**, 163–192 (2007).

[49] Stolpe, M., Stidsen, T.: A hierarchical method for discrete structural topology design problems with local stress and displacement constraints. *International Journal for Numerical Methods in Engineering*, **69**, 1060–1084 (2007).

[50] Stolpe, M., Svanberg, K.: Modelling topology optimization problems as linear mixed 0–1 programs. *International Journal for Numerical Methods in Engineering*, **57**, 723–739 (2003).

[51] Svanberg, K., Werme, M.: Sequential integer programming methods for stress constrained topology optimization. *Structural and Multidisciplinary Optimization*, **34**, 277–299 (2007).

[52] van Dijk, N.P., Yoon, G.H., van Keulen, F., Langelaar, M.: A level-set based topology optimization using the element connectivity parameterization method. *Structural and Multidisciplinary Optimization*, **42**, 269–282 (2010).

[53] Wang, M.Y., Chen, S., Wang, X., Mei, Y.: Design of multimaterial compliant mechanisms using level-set methods. *Journal of Mechanical Design (ASME)*, **127**, 941–956 (2005).

[54] Yamada, T., Yamasaki, S., Nishiwaki, S., Izui, K., Yoshimura, M.: Design of compliant thermal actuators using structural optimization based on the level set method. *Journal of Computing and Information Science in Engineering (ASME)*, **11**, 011005 (2011).

[55] Yamasaki, S., Kawamoto, A., Nomura, T.: Compliant mechanism design based on the level set and arbitrary Lagrangian Eulerian methods. *Structural and Multidisciplinary Optimization*, **46**, 343–354 (2012).

[56] Yoon, G.H.: Maximizing the fundamental eigenfrequency of geometrically nonlinear structures by topology optimization based on element connectivity parameterization. *Computers and Structures*, **88**, 120–133 (2010).

[57] Yoon, G.H., Joung, Y.S., Kim, Y.Y.: Optimal layout design of three-dimensional geometrically non-linear structures using the element connectivity parameterization method. *International Journal for Numerical Methods in Engineering*, **69**, 1278–1304 (2007).

[58] Yoon, G.H., Kim, Y.Y.: Element connectivity parameterization for topology optimization of geometrically nonlinear structures. *International Journal of Solids and Structures*, **42**, 1983–2009 (2005).

[59] Yoon, G.H., Kim, Y.Y., Bendsøe, M.P., Sigmund, O.: Hinge-free topology optimization with embedded translation-invariant differentiable wavelet shrinkage. *Structural and Multidisciplinary Optimization*, **27**, 139–150 (2004).

[60] Yoon, G.H., Kim, Y.Y., Langelaar, M., van Keulen, F.: Theoretical aspects of the internal element connectivity parameterization approach for topology optimization. *International Journal for Numerical Methods in Engineering*, **76**, 775–797 (2008).

[61] Yoon, G.H., Noh, J.Y., Kim, Y.Y.: Topology optimization of geometrically nonlinear structures tracing given load-displacement curves. *Journal of Mechanics of Materials and Structures*, **6**, 605–625 (2011).

[62] Zhou, H., Mandala, A.R.: Topology optimization of compliant mechanisms using the improved quadrilateral discretization model. *Journal of Mechanisms and Robotics (ASME)*, **4**, 021007 (2012).

[63] Zhu, B., Zhang, X., Wang, N.: Topology optimization of hinge-free compliant mechanisms with multiple outputs using level set method. *Structural and Multidisciplinary Optimization*, **47**, 659–672 (2013).